Published in final edited form as:
J Hum Evol. 2013 April ; 64(4): 263–279. doi:10.1016/j.jhevol.2012.12.003.

A volumetric comparison of the insular cortex and its subregions in primates

Amy L. Bauernfeind[a,b,*], **Alexandra A. de Sousa**[c], **Tanvi Avasthi**[b], **Seth D. Dobson**[d], **Mary Ann Raghanti**[e], **Albert H. Lewandowski**[f], **Karl Zilles**[g,h], **Katerina Semendeferi**[i], **John M. Allman**[j], **Arthur D. (Bud) Craig**[k], **Patrick R. Hof**[l,m], and **Chet C. Sherwood**[b]

[a]Department of Anthropology, Hominid Paleobiology Doctoral Program, The George Washington University, Washington, DC 20052, USA

[b]Department of Anthropology, The George Washington University, Washington, DC 20052, USA

[c]Department of Life Sciences, Forensic Sciences Center, University of Coimbra, 3001-401 Coimbra, Portugal

[d]Department of Anthropology, Dartmouth College, Dartmouth, NH 03755, USA

[e]Department of Anthropology and School of Biomedical Sciences, Kent State University, Kent, OH 44242, USA

[f]Cleveland Metroparks Zoo, Cleveland, OH 44109, USA

[g]Institute of Neuroscience and Medicine INM-1, Research Center Jülich, D-52525 Jülich, Germany

[h]C. and O. Vogt Institute of Brain Research, Heinrich Heine University, Düsseldorf, D-40225 Düsseldorf, Germany

[i]Department of Anthropology, University of California San Diego, La Jolla, CA 92093, USA

[j]Division of Biology, California Institute of Technology, Pasadena, CA 91125, USA

[k]Atkinson Research Laboratory, Barrow Neurological Institute, Phoenix, AZ 85041, USA

[l]Fishberg Department of Neuroscience and Friedman Brain Institute, Icahn School of Medicine at Mount Sinai, New York, NY 10029, USA

[m]New York Consortium in Evolutionary Primatology, New York, USA

Abstract

The neuronal composition of the insula in primates displays a gradient, transitioning from granular neocortex in the posterior-dorsal insula to agranular neocortex in the anterior-ventral insula with an intermediate zone of dysgranularity. Additionally, apes and humans exhibit a distinctive subdomain in the agranular insula, the frontoinsular cortex (FI), defined by the presence of clusters of von Economo neurons (VENs). Studies in humans indicate that the ventral anterior insula, including agranular insular cortex and FI, is involved in social awareness, and that the posterodorsal insula, including granular and dysgranular cortices, produces an internal representation of the body's homeostatic state. We examined the volumes of these cytoarchitectural areas of insular cortex in 30 primate species, including the volume of FI in apes and humans. Results indicate that the whole insula scales hyperallometrically (exponent = 1.13) relative to total brain mass, and the agranular insula (including FI) scales against total brain mass

*Corresponding author. amy81@gwu.edu (A.L. Bauernfeind).

with even greater positive allometry (exponent = 1.23), providing a potential neural basis for enhancement of social cognition in association with increased brain size. The relative volumes of the subdivisions of the insular cortex, after controlling for total brain volume, are not correlated with species typical social group size. Although its size is predicted by primate-wide allometric scaling patterns, we found that the absolute volume of the left and right agranular insula and left FI are among the most differentially expanded of the human cerebral cortex compared to our closest living relative, the chimpanzee.

Keywords

Allometry; Brain; Evolution; Frontoinsular cortex; Hominoids

Introduction

The insular cortex is located on the lateral wall of the cerebral hemispheres of mammals, overlying the claustrum, and interposed between the piriform, orbital, motor, sensory, and higher-order auditory cortices (Türe et al., 1999). Most primates have enlarged parietal and temporal opercula, and the insular cortex is hidden from view within the depths of the Sylvian fissure. In other primates where the Sylvian fissure is not as well developed (e.g., *Perodicticus*, *Galagoides*, *Loris*), the insula may be exposed on the brain's lateral surface (Preuss and Goldman-Rakic, 1991). The insula is interconnected with anterior cingulate cortex, rostral and dorsolateral prefrontal cortex, regions of the parietal and temporal lobes, as well as entorhinal cortex, amygdala, hypothalamus, and dorsal thalamus, and it is involved in viscerosensory, visceromotor, somatosensory, and interoceptive functions (Price, 1999; Critchley, 2005). Human functional neuroimaging studies show activation of the insula in association with an individual's emotional state that seems to reflect an internal representation of the body, providing a potential neurobiological basis for subjective awareness useful in the guidance of social interactions (Craig, 2002, 2009; Singer et al., 2009). Specifically, the human insular cortex is important for self-recognition, awareness of emotions, time perception, empathy, and decision-making under uncertainty, as well as the processing of music and language. It has been hypothesized that human cognitive evolution was accompanied by changes in capacities that rely on insula function, such as intersubjective perspective-taking, cooperation, and empathy (Singer et al., 2004; Craig, 2009). However, the neural structures that subserve such psychological specializations in our lineage remain unclear. Given the importance of the insular cortex for sociocognitive processing, the purpose of the current study was to examine the relative size of the insula and its constituent cytoarchitectural subdivisions in humans and other primates.

The primate insular cortex may be divided into three cytoarchitectural subregions based on the distinctiveness of granularity in cortical layer IV, defined by the presence of small, densely packed neurons (Rose, 1928; Mesulam and Mufson, 1982; Carmichael and Price, 1994; Öngür et al., 2003; Kurth et al., 2010a; Gallay et al., 2011). Accordingly, the cellular composition of the insula displays a gradient, transitioning from granular neocortex in the posterior and dorsal insula to agranular neocortex in the anterior and ventral insula, with an extensive intermediate zone of dysgranularity. In addition to the three sectors of insula that can be recognized in all primates, great apes and humans exhibit a distinctive subdivision of agranular insular cortex, frontoinsular cortex (FI), located within the most ventral anterior part of the agranular insular cortex adjacent to the orbital cortex. The FI is defined by the presence of clusters of von Economo neurons (VENs) in cortical layer Vb (von Economo, 1926; Allman et al., 2010). The VENs, which can also be found in the anterior cingulate and dorsolateral prefrontal cortex of humans and great apes, are large spindle-shaped projection neurons with a single basal dendrite (Nimchinsky et al., 1995, 1999; Fajardo et al., 2008).

Data from functional magnetic resonance imaging (fMRI) studies in humans suggest that anatomical variation in the cytoarchitecture of insular cortex may correspond to functionally distinct areas. Specifically, the posterior insula displays activation in the processing of thermosensory information, pain, hunger, thirst, and touch in a somatotopically organized posterior-to-anterior (foot to mouth) gradient (Ostrowsky et al., 2002; Craig, 2003, 2010). The more anterior regions of the insula, likely including agranular insular cortex and FI, complement the posterior insula's representation of one's body state with the ability to process subjective feelings and social awareness. For example, the sensation of pain in one's own body activates posterior insula, whereas feeling empathy for another's pain activates the anterior insula (Singer et al., 2004). Although imaging studies cannot provide direct correspondence between function and cytoarchitecture, different functions have been ascribed to the posterodorsal insular cortex, consisting of mostly granular and dysgranular cortices, versus the ventral anterior insular cortex, which is composed of agranular cortex and FI (Wager and Barrett, 2004; Mutschler et al., 2009; Kurth et al., 2010b). Further supporting the notion that the anterior insular cortex is important for social awareness, it is notable that a severe loss of VENs and widespread degeneration of this region are observed in human patients with the behavioral variant of fronto-temporal dementia, a disease that impairs the individual's ability to recognize the impact of his or her actions on other's emotions (Seeley et al., 2006; Kim et al., 2012). A reduction of VENs within ACC and FI also occurs in human patients with agenesis of the corpus callosum, a condition that is linked to impoverished understanding of one's emotions and difficulty understanding the emotional states of others (Kaufman et al., 2008). Additionally, a greater number of VENs are present in the FI of autistic children, a finding that may relate to the enhanced interoception reported in these individuals (Santos et al., 2011).

It is also notable that left and right anterior insula display functional differences. Several studies have shown predominant activation of right anterior insula during arousing feelings with negative emotional valence and sympathetic activation, while approach behavior, positive affect, and parasympathetic function may associate predominantly with left anterior insula activation (Craig et al., 2000; Critchley et al., 2004; Craig, 2005). These opponent processes are thought to work in concert to provide a homeostatic balance and unified sense of awareness.

In the current study, we examined phylogenetic variation in the volume of insular cortex subdivisions. Such an approach is rooted in Jerison's (1973) principle of proper mass, which states that the volume of a particular cortical area is proportional, 'to the amount of information processing involved in performing the function'. As the volume of a region expands, the number of neurons and local connections within the region increases (Kaas, 2000), enhancing the fine-tuned processing of the functional output. The capacity for information processing of this nature might be particularly critical for regions underlying social interaction (Dunbar, 1998; Barton, 2006), including the anterior insular cortex (Lamm and Singer, 2010).

Although the volume of insular cortex has previously been measured in humans and apes using structural MRI (Semendeferi and Damasio, 2000), the volumetric extent of the cytoarchitectural subregions that comprise the insular cortex have not yet been examined. Moreover, quantitative data on the insular cortex are lacking from other species of primates beyond hominoids. In this study, we present new volumetric measurements of the insular cortex based on cytoarchitectural analysis from 30 primate species. We examined the allometric scaling of insular cortex and its subdivisions relative to brain size to determine whether the volume of agranular insula, including that containing FI in hominids, has increased in humans or any other primate clade. Additionally, we investigated whether the volume of insular cortex or any of its subdivisions are relatively expanded in species that

live in larger social groups. Lastly, because the insula displays functional lateralization, we explored whether hemispheric asymmetry in the volume of the insular cortex is present among humans and great apes. In studying the relative size of these insular subregions across primates, we aimed to provide insight into the neural basis of specialized functions in social cognition.

Methods

Specimens

The sample used in this study consisted of 43 brain specimens from 30 different primate species (Fig. 1). The sample included representatives of strepsirrhines ($n = 6$), platyrrhines ($n = 8$), cercopithecoids ($n = 7$), and hylobatids ($n = 3$). The hominid sample included specimens from *Homo sapiens* ($n = 5$), *Pan troglodytes* ($n = 3$), *Pan paniscus* ($n = 3$), *Gorilla gorilla* ($n = 4$), *Pongo pygmaeus* ($n = 2$), and *Pongo abelii* ($n = 2$). The mass of the whole brain following initial fixation was available from every specimen and was a prerequisite for inclusion in this study. A complete list of specimens, including sex and age, is shown in Table 1.

Volumetric measurement methodology

To collect measurements in the greatest possible range of primate species, our sample consisted of specimens from several collections, including those from the Great Ape Aging Project (GAAP), the Stephan comparative neuroanatomy collection at C. & O. Vogt Institute of Brain Research in Düsseldorf, Germany, the Welker collection at the National Museum of Health and Medicine in Washington, DC, and the University of California, San Diego (UCSD). The details of fixation, embedding, sectioning, and Nissl staining differed across these collections and have been described previously in other publications (Allman et al., 2010; de Sousa et al., 2010; Semendeferi et al., 2010).

Measurements of insular cortex subregions were performed on Nissl-stained coronal sections (see below for details). Volumes of granular, dysgranular, and agranular insular cortices were estimated in the left hemispheres of all specimens. Gallay et al. (2011) noted gradations in granularity (as seen in Nissl staining) that would divide the insula into more than three principle regions. In contrast, we tracked the volume of the three principle regions alone. While variations exist in the pattern of granularity within the three principle insular subdivisions, the variation is clearly inter-regional and does not detract from the identifications of the three principle regions. Without the assistance of several immunohistochemical stains, we found that additional parcellations cannot be consistently and confidently identified across species. We therefore limited our consideration to agranular, dysgranular, and granular insular cortices, which can be identified through Nissl staining alone.

Volume estimation of the subdivisions of insular cortex was performed by C.C.S. and A.L.B. according to the granularity (density of cells) within layer IV and was in agreement with the classifications of granularity used in other studies (Mesulam and Mufson, 1982; Carmichael and Price, 1994; Öngür et al., 2003; Gallay et al., 2011). To assess reliability between the two observers, volumes for subdivisions of insular cortex were estimated on six of the same specimens. Inter-observer reliability was high for each region measured: total insular volume ($r = 0.92$, $p = 0.010$), granular ($r = 0.88$, $p = 0.021$), dysgranular ($r = 0.82$, $p = 0.044$), and agranular ($r = 0.82$, $p = 0.048$) insular cortices. In great apes and humans, the volume of FI was estimated when VENs were present in clusters. Additionally, when the tissue was available, the volumes of both right and left insulae were estimated in great apes and humans to allow for interhemispheric volume comparison.

Sections from a subset of specimens (as indicated in Table 1) were examined at regularly spaced intervals through the length of insular cortex and boundaries of subregions were manually drawn using StereoInvestigator software (MBF Bioscience, Williston, VT). The Cavalieri principle was used to calculate the volume of each region based on the areas of the regions traced and the interval thickness. Sections from the remaining specimens were scanned on a flatbed scanner at 2400 dpi and were evaluated at regular intervals through the length of insular cortex in ImageJ 1.42q software (http://rsb.info.nih.gov/ij/). Using the cell counting plug-in, an estimate of volume was obtained by counting the number of markers corresponding to each insular subregion that intersected a grid overlay (ranging from 20 to 200 μm depending on brain size). The number of markers placed per subregion was totaled across all sections containing insula and multiplied by the grid spacing and interval thickness to obtain an estimation of volume. We measured the entire gray matter of the cortex, extending from the pial surface to the bottom of layer VI at its interface with the white matter.

To account for the shrinkage that occurs following histological processing, we calculated correction factors for all specimens according to the method described by de Sousa et al. (2010). Several of the specimens from the GAAP collection were sectioned as separate blocks, and a correction factor was calculated for each block individually. The correction factor is the quotient of the preprocessed brain volume and the volume of the same brain after histological processing. To calculate the preprocessed brain volume, brain mass was divided by the specific gravity of brain tissue (1.036 g/cm^3; Stephan, 1960). To calculate the postprocessing volume, images of sections were obtained using a flatbed scanner at 600 dpi and the total planimetric area of the scanned sections was obtained using ImageJ. All estimates of the volume of insular cortex and its subregions were multiplied by the brain-specific correction factor to account for shrinkage from histological processing.

Anatomical definition of insular cortex

Many investigators have distinguished insula from surrounding cortices and identified distinct subregions based on multiple staining procedures in primate species including galagos (Preuss and Goldman-Rakic, 1991), macaques (Mesulam and Mufson, 1982; Preuss and Goldman-Rakic,1991; Carmichael and Price,1994; Gallay et al., 2011), and humans (Öngür et al., 2003; Kurth et al., 2010a). Taken collectively, these studies indicate that the parcellation of insular cortex from surrounding cortical regions is possible across primate taxa. Additionally, major cytoarchitectural subregions, including granular, dysgranular, and agranular insular cortices, are consistent across primates (Fig. 2 B and C), although identification of additional subdivisions may be possible (Rose,1928; Carmichael and Price, 1994; Öngür et al., 2003; Gallay et al., 2011). In this study, we adopt the methodology used by Mesulam and Mufson (1982) in dividing the insula into granular, dysgranular, and agranular cortices because these subdivisions are clearly identifiable in Nissl-stained sections across all primate species examined.

Superior and inferior boundaries—In most primate species, the insula is contained within the Sylvian fissure and is bounded by its two offshoots, the superior limiting sulcus (SLS) and the inferior limiting sulcus (ILS). Many strepsirrhine species do not have an SLS branch of the Sylvian fissure comparable with to that seen in anthropoids. Nonetheless, an incipient homolog of the SLS can be identified as a dimple or bend in the cortical surface. All specimens lacking a well-developed Sylvian fissure had this feature. The SLS, or its homologous dimple in the cortical surface, was used to mark the dorsal extent of insular cortex (Figs. 3 and 4).

The inferior boundary is defined differently, depending on the antero-posterior position of the coronal section relative to the *limen insulae* (see below). The *limen insulae* is the junction of the temporal lobe with the ventral insular cortex (Mesulam and Mufson, 1982).

Anterior to the *limen insulae*—Mesulam and Mufson (1982) describe the most anterior extent of the insula in macaques as coincident with the appearance of the SLS in posterior orbitofrontal cortex (Fig. 3A,B and 4A). Strepsirrhine species typically lack a well-developed SLS anterior to the *limen insulae*, and the homologous dimple on the lateral surface of the cortex marked the beginning of insular cortex in these species (Fig. 4B). At this coronal level, the insula lacks the clear ventral border offered by the ILS of the more posterior insula. Although a clearer anterior limiting sulcus (ALS) may be distinguished in humans, this is not a landmark seen in most primates. Consequently, the ventral boundary of insular cortex must be distinguished from surrounding orbitofrontal cortex based on cytoarchitecture. The ventromedial border of insula has been shown to be superficial to the medial extent of the claustrum (Preuss and Goldman-Rakic, 1991; Carmichael and Price, 1994; Öngür et al., 2003). Therefore, we used the ventromedial termination of the claustrum to indicate the transition of insula to orbitofrontal cortex in anthropoids. In strepsirrhine primates that lack an extensive orbitofrontal cortex, ventral anterior insula fully extends to the piriform cortex (Fig. 4B; Preuss and Goldman-Rakic, 1991). In all specimens studied, the ventral extent of the anterior insular cortex is either agranular or dysgranular in composition. In the remainder of the insula anterior to the *limen insulae*, granular cortex may occur dorsally, but the anterior insula is usually comprised of dysgranular and agranular cortices. A larger amount of agranular cortex typically occurs in the ventral insula nearer the *limen insulae* than in more anterior levels.

At the limen insulae—At this location the temporal lobe meets the ventral insular cortex, and the piriform cortex trifurcates into parts, which extend into orbital cortex, insula, and the medial temporal lobe (Mesulam and Mufson, 1982). In Nissl-stained preparations, the piriform cortex may be recognized by its lack of granularity and darkly stained pyramidal cell layer. At the *limen insulae* of all species studied, the ventral boundary of insular cortex was defined as the dorsal boundary of the insular branch of the piriform cortex (Figs. 3 and 4; Mesulam and Mufson, 1982; Preuss and Goldman-Rakic, 1991; Gallay et al., 2011).

Posterior to the *limen insulae*—Moving posteriorly away from the *limen insulae*, the insula is composed of a greater proportion of granular and dysgranular cortices. The insular cortex is separated from the somatosensory cortex of the parietal operculum by the SLS and from the auditory cortex of the temporal operculum by the ILS (Naidich et al., 2004). Posterior to the *limen insulae*, the SLS becomes more defined in some strepsirrhine primates (*Avahi laniger*, *Indri indri*, *Varecia variegata*), while a homologous bend in the cortex persists in others (*Perodicticus potto*, *Galagoides demidoff*, *Loris tardigradus*). In the sections approaching the posterior limit of the insula, layer IV is continuous and thick. In most primate species, SLS and ILS clearly define the dorsal and ventral borders of the insula, and the convergence of these two sulci defines its posterior extent. We used the disappearance of the SLS, or its homolog, to indicate the posterior extent of the insula.

Insula subregional boundaries—Because section thickness can affect how granular layer IV appears, cytoarchitectural regions were identified by comparing the extent of granularity to adjacent regions within a specimen. Although small layer IV neurons may be present in the agranular insular cortex, they are so scarce that the layer is hardly visible. In general, dysgranular cortex abuts the superior limit of agranular cortex and is primarily recognized by the sudden increase in granularity of layer IV. Though small layer IV neurons are apparent in dysgranular cortex, the superficial and deep boundaries of the layer are

obscured. In the dysgranular insula, granularity occurs in cortical layer II to varying degrees. The granular cortex abuts the superior limit of the dysgranular insular cortex and continues into the most posterior and dorsal portions of insular cortex. The densely granular layers II and IV of the granular insular cortex allow these layers to be clearly distinguished and delimited.

The concentration of VENs in great apes and humans allows for a region of ventral anterior agranular insula to be defined as FI. Recently, other researchers have noted the presence of VENs in the anterior insula of the macaque monkey (Evrard et al., 2012). No data currently exist about the density of VENs outside of the hominoid clade, but in our observations, VENs in these species do not cluster. Here, we defined FI based on the clustering the VENs due to the practical concern of defining a subset of agranular insula as FI when only a single VEN or two exist in a discrete region of cortex. In hominoids, VENs were identified under high magnification, and markers were placed to map FI at low magnification. Under low magnification, a region of agranular insula was designated as FI based on the presence of clusters of VENs within a discrete region of cortex (Fig. 3A).

Scaling

Using log-transformed cortical region volumes and brain volumes, we examined the scaling relationships of left insular cortex and its subregions in all species studied (Table 1). Because more than one individual from the great apes and humans were sampled for this study, we calculated mean volumes for those taxa prior to conducting comparisons across primate species. To account for possible effects of autocorrelation, in each analysis we subtracted the volume of the dependent variable from the independent variable before calculating regression coefficients. To examine scaling relationships across primate species, we used reduced major axis regression (RMA) because both x and y variables were expected to be symmetrical and these variables could have contained error (Smith, 2009). In RMA analyses, the residual variance is diminished in both the x and y dimensions, whereas ordinary linear regression only accounts for variance in the y dimension (Sokal and Rohlf, 1995). Because RMA analyses consider residual variance in both dimensions, the effect that fixation may have on brain mass or volume of regions would not alter the RMA slope. All RMA slopes were calculated using (S)MATR software version 1.0 (Falster DS, Warton DI, and Wright IJ; http://www.bio.mq.edu.au/ecology/SMATR). Small within-species sample sizes precluded an analysis of sex differences.

To determine whether the volume of the human insula deviated from predictions based on the scaling relationships of nonhuman primates, we removed the humans from the sample and calculated non-phylogenetic least squares (LS) regression lines for insula and its subdivisions to whole brain volume. An LS line was used to examine departures from allometry because it produces residuals that are uncorrelated with the independent variable (Harvey and Krebs, 1990). A prediction of the volume for each subregion was found based on log–log LS regression. This predicted value was detransformed (from the logarithmic to arithmetic scale) and the quasi-maximum likelihood estimator (Smith, 1993) was used to correct for detransformation bias.

As RMA regression does not account for the relatedness of species and treats all tips of the phylogenetic tree as being equally as likely to share traits, we also included phylogenetic information in our allometric analysis to account for possible phylogenetic dependence among regression residuals (O'Neill and Dobson, 2008; Revell, 2010). Allometric slopes were estimated using a phylogenetic generalized least-square (PGLS) approach (Martins and Hansen, 1997; Pagel, 1999; Martins et al., 2002) implemented in the program BayesTraits (Pagel et al., 2004). This approach incorporates phylogenetic information directly into the regression model by representing the error term as a variance-covariance matrix scaled by

the parameter λ, which is a measure of phylogenetic signal (Freckleton et al., 2002). The λ parameter is estimated from the species data via maximum likelihood and ranges from 0 to 1. When $\lambda = 0$, the results are equivalent to non-phylogenetic LS regression because the internal branches of the tree are collapsed to zero, resulting in a star phylogeny. Values of $\lambda > 0$ represent increasing levels of phylogenetic dependence among the regression residuals, with $\lambda = 1$ indicating no transformation of the branch lengths was used because the error term is perfectly dependent on phylogeny. To take into account phylogenetic uncertainty, we downloaded a sample of 100 primate trees from the 10kTrees website (http://10ktrees.fas.harvard.edu/). The website provides free access to a Bayesian posterior probability distribution of primate phylogenies derived from molecular data (Arnold et al., 2010). We ran each PGLS analysis across the entire tree block so that the results would not be dependent on any one tree or set of branch lengths. A phylogenetic tree displaying the relatedness of our sample appears in Fig. 1.

Because the insula supports cognition relating to complex social interactions, we hypothesized that sociality would affect the volume of the anterior insular cortex subdivisions. Mean group size data collected from published literature (Nunn and van Schaik, 2001; Nunn, 2002, Table 1) were used as a measure of sociality. We used PGLS multiple regression analyses to examine the relationship between the volume of the entire insula and species average social group size, while controlling for total brain size, and the relationship between the volume of each of the four different cytoarchitectural subdivisions of insula (including granular, dys-granular, agranular, and agranular and FI combined) and social group size, while controlling for total brain size.

To determine the relationship of body mass with the volume of insular cortex and its subdivisions, we ran a separate set of PGLS analyses using sex-specific species body mass averages published by Smith and Jungers (1997; Table 1) as a dependent variable. Because most of our sample consists of males, we excluded the females from these analyses. If more than one species mean appeared in the article (either from subspecies or distinct populations), we used an average of the available data. To estimate the body mass of humans, we used the averages from the Danish population (Holloway, 1980), which most closely resembled the humans in western populations sampled by this study. First, the insula as a whole and each of its cytoarchitectural areas were regressed against body mass averages. Using PGLS multiple regression analyses, we examined the relationship of brain volume (after subtracting the volume of the insula) against body mass and group size to determine the influence of these factors on brain volume. Lastly, we analyzed the scaling between the volume of the entire insula and each of its cytoarchitectural areas separately against body mass and group size.

Measurement of asymmetry in great apes and humans

We analyzed volumetric lateral asymmetry of the insular cortex and its subdivisions among great apes and humans in specimens where the left (Table 1) and right (Table 2) hemispheres were available for measurement. The sample in this analysis included *H. sapiens* ($n = 5$), *P. troglodytes* ($n = 2$), *P. paniscus* ($n = 3$), *G. gorilla* ($n = 2$), *P. abelii* ($n = 1$), and *P. pygmaeus* ($n = 1$). Asymmetry quotients (AQ) were used to evaluate lateralization of total insula and its subregions. Asymmetry quotients were calculated using the formula $AQ = (R - L)/[(R + L)/2]$ where L and R are the left and right volumetric estimates for a given region in a single individual. The computation produces positive values for rightward volumetric biases and negative values for leftward volumetric biases.

Results

The relative positions of granular, dysgranular, and agranular insular cortices were nearly identical in all species examined and closely resembled those described by previous studies (Mesulam and Mufson, 1982; Bonthius et al., 2005, Fig. 2). We found the distinctions among the subdivisions of insular cortex provided by Mesulam and Mufson (1982) appropriate across primate species. Examples of parcellations in the coronal plane are displayed for a hominoid (*H. sapiens*), a cercopithecoid (*Macaca maura*), a platyrrhine (*Ateles geoffroyi*), and a strepsirrhine (*L. tardigradus*) in Figs. 3 and 4. The volume estimates of left insular cortex and its subdivisions for each individual appear in Table 1. Table 2 contains the volume estimates for right insula in great apes and humans. We found no individual subdivision of insula to be consistently the largest across primate taxa, but granular and dysgranular insula most frequently occupied the greatest fraction of the insular cortex.

In coronal sections, VENs (Fig. 5A) appeared primarily on the crowns of gyri in the portion of ventral anterior agranular insula that is anterior to the *limen insulae*. Rarely, single VENs were found elsewhere, but because FI is defined by the concentration of VENs, regions containing isolated VENs were not classified as FI. In agreement with recently published literature (Evrard et al., 2012), VENs were found in the ventral anterior insula in species outside of great apes. However, the cells were not clustered, and an FI-like region could not be traced. In most cases, the cortex containing VENs appeared between dysgranular and agranular insular cortices. In cases where VENs were clustered in two or more distinct areas of a coronal section, each discrete region containing VENs was traced and categorized as FI. When this occurred, the cortex between FI regions was always agranular.

Scaling of the left insula across primates

Mean volumes of each subdivision of insular cortex for great apes and humans (Table 3) were combined with volumes from individuals representing other taxa. Linear regressions of the left insula and its cytoarchitectural subdivisions against total brain volume are shown in Fig. 6. In all analyses, RMA and PGLS regressions yielded nearly identical scaling relationships (Fig. 6A–E), and the conclusions drawn from both analyses are similar. This is explained in part by the minimal degree of phylogenetic signal observed among regression residuals (all maximum likelihood λ values were zero).

The scaling of the entire left insula to the volume of the brain revealed a positive allometric relationship (Fig. 6A), meaning that as primate brain size increases the total insula volume tends to increase in size moderately faster than the rest of the brain. The volume of the insula scales to the rest of the brain at a rate of 1.13 (95% CI = 1.05–1.22), revealing that the insula of large-brained primates, including great apes and humans, is between 5% and 22% bigger than predicted by isometry. Granular and dysgranular insular cortices (Fig. 6B, C) increase in size at rates comparable with that of total insula. Because FI is defined as agranular insula that contains clusters of VENs, the combined volume of agranular insula and FI in great apes and humans may be considered comparable with the agranular insula in the taxa where VENs do not cluster. Scaling of agranular insula (Fig. 6D) and agranular insula and FI combined (Fig. 6E) reveal that the anterior portions of insular cortex increase in size at a greater rate than the dysgranular or granular insular cortices. The volume of agranular insula (excluding FI) scales to the rest of the brain at a rate of 1.18 (95% CI = 1.05–1.32), and the volume of agranular insula including FI scales to the rest of the brain at a rate of 1.23 (95% CI = 1.10–1.36).

We also explored how the proportions of insular cortex subdivisions covary with the total size of left insular cortex. The volume of granular insula (RMA $b = 0.94$, 95% CI = 0.83–

1.07, R^2 = 0.89; PGLS b = 0.89, 95% CI = 0.78–1.01, R^2 = 0.90), dysgranular insula (RMA b = 1.02, 95% CI = 0.93–1.11, R^2 = 0.96; PGLS b = 0.99, 95% CI = 0.90–1.08, R^2 = 0.95), agranular insula (RMA b = 1.04, 95% CI = 0.94–1.16, R^2 = 0.93; PGLS b = 1.01, 95% CI = 0.90–1.08, R^2 = 0.93), and agranular insula and FI combined (RMA b = 1.10, 95% CI = 1.00–1.21, R^2 = 0.94; PGLS b = 1.07, 95% CI = 0.97–1.17, R^2 = 0.94) all scaled to the rest of insular cortex at rates that were indistinguishable from isometry.

In addition, we explored how insular cortex size is related to body mass. We found that the scaling of insular cortex against body mass was statistically indistinguishable from that of total brain volume against body mass (Table 4). Therefore, a major factor that governs the size of insular cortex relative to the body is overall brain size.

We examined whether the volume of human insula deviated from predictions based on the scaling relationships of nonhuman primates by removing the humans from the sample and calculating non-phylogenetic least squares (LS) regression lines for insula and its subdivisions against whole brain volume. The percent differences between observed and predicted values are shown in Table 5. For each region, human values fell within the 95% confidence intervals of the nonhuman primate LS regression.

Table 6 lists how the fold-difference between the volume of insula and its subdivisions in the human brain compare with the volume of the same region in *P. troglodytes* and *P. paniscus*, and how the two species of chimpanzee compare to each other. Values from this study are listed alongside those from other cortical regions measured in previous studies for reference.

Group size and insula volume

We examined the correlations between social group size and the volume of the insular cortex and its subdivisions using PGLS multiple regression analyses. There was no significant correlation between the volume of the left insula and group size aftercontrolling for total brain volume (b = −0.02; t = −0.24; p = 0.816). Additionally, no significant correlations were found between group size and the volume of granular (b = 0.07; t = 0.63; p = 0.533), dysgranular (b = −0.02; t = −0.30; p = 0.766), and agranular (b =−0.03; t =−0.27; p = 0.789) insular cortices or the volume of agranular insula and FI together (b = −0.02; t = −0.16; p = 0.875) after controlling for total brain volume. The results were the same when catarrhines were analyzed separately from the rest of the primate sample.

For the male specimens of our sample, we also examined the correlations between social group size and the volume of the insular cortex and its subdivisions using PGLS multiple regression analyses while controlling for body mass. A significant correlation was found between the volume of the left insula and group size after controlling for body mass (b = 0.13; t = 4.11; p < 0.001). Additionally, significant correlations were found between group size and the volume of granular (b = 0.15; t = 2.97; p = 0.007), dysgranular (b = 0.15; t = 3.16; p = 0.004), and agranular (b = 0.17; t = 3.17; p = 0.004) insular cortices, as well as the volume of agranular insula and FI together (b = 0.17; t = 3.34; p = 0.003) after controlling for body mass. These data show that, independent of body mass, the volume of the insula and each of its subdivisions is tightly correlated with group size.

Asymmetry of insula in humans and great apes

The volume of each insula subdivision from the left and right hemispheres of humans and great apes are shown in Tables 1 and 2, respectively. Asymmetry quotients are plotted in Fig. 7 for each specimen in which the volume of both the left and right insulae could be measured. Within each species, volumetric asymmetry across the insula as a whole and each

of its subdivisions were examined by one-sample *t*-tests. No region in any species displayed a significant difference in volume between hemispheres.

Discussion

Imaging studies examining the neurobiological underpinnings of human-specific social cognition have consistently found that the ventral anterior insula is activated during cognitive tasks associated with the awareness of autonomic changes and emotion that underlie the regulation of interpersonal relationships (meta-analysis in Mutschler et al., 2009). Accordingly, we predicted that the volume of agranular insula and FI would be larger as a reflection of specializations in humans and other primates living in complex social systems. In support of this expectation, we found that agranular insula and FI display positive allometric scaling across primates. Therefore, relative increase in the size of the ventral anterior insula (including agranular insular cortex and FI) accompanies brain enlargement in primates and might contribute to adaptive specializations for sociality. Notably, however, after taking allometric scaling for brain size into account, additional variation in the volume of insular cortex regions in primates did not correlate with social group size. However, the correlations between regional insular cortex volumes and social group size were highly significant after correcting for only body size. Because we find that total insula volume is tightly linked to brain size as a whole, these results are expected since brain size expands rapidly with increases in social group size (Dunbar and Schultz, 2007).

Size and scaling of insula and subdivisions

It was previously found based on measurements of MRIs that both right and left human insulae, including cortex and immediately underlying white matter (external capsule), occupy a total of 17.4 cm^3 (Semendeferi and Damasio, 2000). We found that the average total insular cortical volume from both hemispheres in humans (Tables 1 and 2) in the present study is somewhat lower than reported above, namely 12.7 cm^3. Estimates of total insular volume in the present study are less than those found by Semendeferi and Damasio (2000) for all species sampled (Tables 1 and 2). A difference in the anatomical definition of insular cortex (i.e., indicating the extreme capsule as the medial border of the insula compared with the lower boundary of layer VI) certainly contributes to the discrepancy.

In this study, the majority of the log interspecific variability (97% predicted by RMA scaling) of the volume of insula was explained by total brain size. Likewise, each subdivision of insular cortex was closely linked to size of the insula as a whole (RMA R^2 = 0.89 and greater). Humans did not deviate from the allometric scaling predictions based on the volumes of these regions in other primates. These results suggest that the size of the insula and its subdivisions in humans – and in all primates studied here – reflect adherence to strict scaling laws rather than mosaic adaptive specialization. Dysgranular, granular, and agranular insula (in hominids, the portion that does not include FI) scaled at, or near, isometry (Fig. 6B–D) in primates. However, the anterior insula and FI were between 10% and 36% larger in primates with larger brains, including humans and great apes, than if these regions had enlarged in the same proportion as the rest of the brain (RMA b = 1.23, 95% CI = 1.10–1.36, Fig. 6E). These results indicate that the anterior portions of insular cortex are disproportionately enlarged in association with overall brain expansion in primates. This is similar to the frontal cortex, which also hyperscales in primates as compared with non-frontal regions (Bush and Allman, 2004; Smaers et al., 2010), showing a particularly steep increase in the most rostral regions of the prefrontal cortex in the left hemisphere (Smaers et al., 2011).

While these scaling regularities across primates reveal that the major determinant of insular cortex size is overall brain size, we sought to understand how this might translate to

reorganization among areas in human neocortical evolution. We found that the absolute volumetric size difference between humans and *P. troglodytes* in the left and right agranular insulae and left FI is more pronounced than any other cortical region previously measured, including regions of the prefrontal cortex (Brodmann's areas 10, 44, and 45) (Amunts et al., 1999; Semendeferi et al., 2001; Schenker et al., 2010). Such comparisons of volumetric differences between modern human and chimpanzee brains, however, should not be interpreted to reflect only the differential enlargement of cortical areas in the course of human evolution. Chimpanzee brains do not represent the ancestral state from which humans evolved and there has been significant evolution along the chimpanzee lineage since they shared a last common ancestor with humans (Cáceres et al., 2003; Preuss et al., 2004; Uddin et al., 2004). Indeed, a comparison of insular cortex between chimpanzees and bonobos reveals important neuroanatomical differences between these close relatives of humans. Although panins (*P. troglodytes* and *P. paniscus*) diverged from humans 5–6 million years ago (Goodman et al., 1990) and from each other 1.5 million years ago (Becquet et al., 2007; Hey, 2010), each species has a unique evolutionary history and has a distinctive pattern of social behavior. Notably, our results indicate that bilaterally the agranular insula and FI are considerably larger in *P. paniscus* compared to *P. troglodytes*, a finding that is unique considering that many of the other regions that have been studied are roughly equivalent in volume between the two species.

Previous research in humans has found that the size of the right agranular insula is directly correlated with the degree of subjective awareness an individual has of their own emotional state (Craig, 2004; Critchley et al., 2004). Our data support the conclusion that right agranular insula is expanded in humans, relative to chimpanzees, potentially supporting an enhanced ability to utilize subjective feeling states in applying empathy toward others, enhancing prosocial behaviors. This finding is consistent with the suggestion that modern human societies are remarkable as compared to other primates in the degree of cooperative behaviors that are performed within networks of reciprocal exchange among non-kin, involving food sharing and division of labor (Silk and House, 2011). However, this result cannot be attributed only to an increase in volume of agranular insula in the hominin lineage (leading to humans) but also to a substantial relative decrease in volume of the agranular insula of *P. troglodytes*, as evidenced by the large negative residual of this species (Studentized residual from LS line = −1.18). It is also worth noting that the volume of FI in *P. troglodytes* is much smaller on the left than on the right, an asymmetry that does not characterize any other hominoid species in our dataset. The left hemisphere has been associated with parasympathetic activation and nurturing behaviors, and the right with sympathetic activation and challenge behaviors (Craig, 2005; MacNeilage et al., 2009). Therefore, the smaller volume of left FI in *P. troglodytes* is a potential neural correlate of the more aggressive behavior demonstrated by some members of this species (Wrangham et al., 2006; Townsend et al., 2007; Mitani et al., 2010). Notably, a recent MRI voxel-based morphometry study by Rilling et al. (2011) found the right anterior insula of *P. paniscus* to be enlarged relative to *P. troglodytes*. Considering that brain size in these species is roughly similar, our data from the ventral anterior regions of agranular insula and FI support these findings, suggesting that the enlargement of the right anterior insula of *P. paniscus* might be related to adaptations for risk-aversion behavioral strategies.

The humans in our sample (n =5) displayed a considerable amount of within-species variability in the volume of insula and its subdivisions. The potential remains for individual factors, such as social intelligence, to contribute to the variability of insular cortex subdivisions in the human and nonhuman subjects included in our study.

Social complexity and insula size

We found no significant associations in our multiple regression PGLS analyses of social group size with the volume of insular cortex or any of its cytoarchitecturally defined subdivisions, after controlling for overall brain size. On the other hand, insula and its subdivisions were significantly correlated with group size independent of body mass. The difference in results is due to the high degree of collinearity between body and brain size ($r = 0.65$, $p < 0.001$).

While our findings suggest that insula and its anterior agranular subdivisions are disproportionately enlarged in primates concomitant with increasing brain size, additional variation in insular cortex size beyond allometric scaling did not correlate with social group size. This finding might seem surprising in light of the fact that a large-scale meta-analysis of many hundreds of functional imaging studies strongly implicates the ventral anterior insula in social behavior (Kurth et al., 2010b). Therefore, we propose that the predictable relative enlargement of the insula that accompanies brain expansion may be sufficient to accommodate the information processing demands associated with increased complexity of social groups (Dunbar, 1998; Dunbar and Schultz, 2007). Heteromodal association areas of the neocortex tend to scale up with brain size more rapidly than primary sensory and motor areas in primates (Preuss, 2000). Similarly, the relative increase in insular cortex size, especially in anterior agranular regions, might represent a magnified representation of social awareness compared with neocortical regions involved in unimodal sensory processes. As a consequence, cortical reorganization of the insula that is governed by scaling regularities in primates might help to explain the correlation that has been observed between total brain size and social group size (Charvet and Finlay, 2012). Alternatively, it must be considered that additional subdivisions of insular cortex not measured in this study may reveal a correlation between group size and the volume of an insular subdivision.

Histological organization of insular cortex

All primates exhibit the same basic cytoarchitectural organization of the insula, with granular neocortex located in the posterodorsal insula, which transitions to agranular neocortex in the ventral anterior insula, with an intermediate zone of dysgranular neocortex situated between these two regions (Rose, 1928; Mesulam and Mufson, 1982; Gallay et al., 2011). However, other investigations have found a more complex network of subregions within insular cortex based on gradations of histochemical and immunohistochemical staining. Carmichael and Price (1994) parcellated the macaque insular cortex (*Macaca nemestrina*, *Macaca fascicularis*, and *Macaca mulatta*) into seven subdivisions, identifying granular and dysgranular regions and five variations of agranular cortex. These authors distinguished these areas based on topographic location, cytoarchitecture, the organization of myelinated fibers, and variation in staining for acetylcholine esterase, calbindin, parvalbumin, and nonphosphorylated neurofilament protein. Similar subdivisions were found to exist in the human anterior insula (Öngür et al., 2003). More recently, the macaque (*M. nemestrina* and *M. fascicularis*) insula has been divided into an even greater number of subdivisions based on a similar series of staining procedures (Gallay et al., 2011). No evidence exists as to whether these additional parcellations can be recognized in all primate taxa.

In the current study, we limited our investigation to the three main cytoarchitectural domains that are clearly identifiable using Nissl staining alone. Because the aim of the current study was to include a broad range of primate species, many of which could only be studied from archival slide collections, we were limited in examining only the most clearly defined subdivisions of the insular cortex that can be identified from Nissl-stained preparations. As noted above, dividing the insula into a greater number of areas is certainly possible.

However, such additional parcellation requires methods such as immunohistochemical staining or computerized analysis of cytoarchitecture using measurement of the gray level index (GLI), an approach which compares the distribution cell surface areas across the layers of the cortex (Schleicher et al., 2005; Kurth et al., 2010a). Analysis of cortical area subdivision with GLI data is not readily optimized for use across multiple species.

Interestingly, a broader comparative examination of mammalian species demonstrates a large degree of diversity in insular cortex cytoarchitecture and cellular composition that may underlie specializations in physiology or cognition (Butti and Hof, 2010). For example, many mammalian species, including the sheep (Rose, 1928), the bull (Russo et al., 2008), cetaceans (Hof and Van der Gucht, 2007; Butti and Hof, 2010) and hippopotamuses (Butti and Hof, 2010), lack granular or dysgranular cortices in their insula altogether, a specialization in these species that has been hypothesized to support the unique gastroenteric function of these poly-gastric mammals (Russo et al., 2008; Butti and Hof, 2010). However, the insular cortices of manatees are completely agranular in composition despite the fact that they are monogastric (Butti and Hof, 2010), allowing for the possibility that the lack of granularity within the insular cortex in these species exemplifies a reorganization of cortical structure not related to digestion. At present, little is known about the adaptive advantage of granularity within the insular cortex, including what the functional significance of further subdivisions (beyond agranular, dysgranular, and granular cortices) may be within the species where such cytoarchitectural distinctions are possible (Carmichael and Price, 1994; Öngür et al., 2003; Gallay et al., 2011).

Interconnectivity of insular cortex

Recent studies have demonstrated significant variation in the connectivity of insular cortex across its functionally distinct regions. Human posterior granular insula has been analyzed using measurement of GLI (Kurth et al., 2010a). Findings revealed two areas of posterodorsal granular insula with distinct GLI profiles, indicating that posterodorsal insula of humans may also be divided into more functionally distinct regions than are represented in the current study. Additionally, Golgi staining within the insula of humans has revealed heterogeneity in the dendritic length and spine density of pyramidal neurons in regions that correspond to dysgranular and granular insula (Anderson et al., 2009). These measures are often used as a proxy for cortical interconnectivity and have been found to be elevated in multimodal cortical areas compared with unimodal regions (Jacobs et al., 2001; Elston et al., 2006), indicating that neurons in these areas may be structurally specialized to synthesize a broad range of inputs.

It has been hypothesized that brain regions that become enlarged in the course of evolution may establish a wider range of connectivity through competitive axon sorting in development (Deacon, 1990; Striedter, 2005). Our findings suggest that the allometrically increased size of the agranular insular cortex and FI may accordingly represent a higher degree of connectivity. Therefore, future studies concerning the evolution of the neural underpinnings of social cognition should be directed toward understanding how changes in the connectivity of the insula may contribute to the emergence of an integrated representation of emotion in self and others.

Anterior insula and the distribution of VENs within FI

It has been hypothesized that VENs in the ventral anterior insula may play a key role in emotional and social cognitive differences among humans and other primates (Allman et al., 2010). A previous study in great apes and humans found a higher number of VENs in the right ventral anterior insula compared to the left (Allman et al., 2010). This finding appears consistent with evidence from fMRI indicating that the spatial extent of neural activation in

the right insula of humans is greater than the activation in the left insula during tasks of interoceptive attention (Critchley et al., 2004). In the majority of humans sampled in the current study, we found a leftward asymmetry in the volume of FI, which could possibly contribute to the controlled breathing during speech vocalization in humans (Ackermann and Riecker, 2010). Although we did not perform stereologic counts of total VEN number in this study, when considered alongside the previous data of total VEN counts, it appears that the density of VENs within the human right FI is greater than the left FI. However, in our analyses when agranular insula and FI volumes are combined, a slight rightward asymmetry (non-significant) exists, which is consistent with volumetric data from a previous structural MRI study (Watkins et al., 2001).

Additional data concerning the distribution of VENs in the neo-cortex across mammals will help to clarify their role in the evolution of social cognition. Small numbers of VENs have been reported in cercopithecoids (Rose,1928; Forro et al., 2011; Evrard et al., 2012), at least one genus of platyrrhines (*Ateles*; Evrard et al., 2011), and a strepsirrhine (*Lemur catta*; Rose,1928). VENs have also been found in other mammalian lineages including cetartiodactyls and elephants, suggesting that they may be particularly numerous in insular cortex and anterior cingulate cortex of large-brained, social mammals (Hof and Van der Gucht, 2007; Butti et al., 2009; Hakeem et al., 2009; Butti and Hof, 2010; Butti et al., 2013).

Conclusion

The current study represents the first volumetric comparison of the primate insular cortex based on cytoarchitecture. These data enrich our understanding of how variation in the size of the insular cortex and its subdivisions might contribute to the evolution of emotional and social cognitive functions in primates. We found that left and right agranular insula and left FI of humans are among the most enlarged cortical areas relative to the chimpanzee, although these differences are not as great when comparing humans to bonobos. Differences in the size of these ventral anterior insular regions may underlie cognitive specializations important for the evolution of complex social interactions that have been amplified in the human lineage, such as increased empathy, cooperation, understanding of other individual's mental states, and language (Singer et al., 2004, 2006, 2009; Rilling et al., 2008; Ackermann and Riecker, 2010; Rilling and Sanfey, 2011).

Acknowledgments

The authors thank Archibald Fobbs, curator of the Yakovlev and Welker Brain Collections and Dr. Adrianne NOE, director of the National Museum of Health and Medicine, for making the collections available to us and to the broader scientific community. We thank Joseph M. Erwin and The Great Ape Aging Project for providing access to many of the brains used in this study. This work was supported by the National Science Foundation (DGE-0801634, BCS-0824531, BCS-0549117), the National Institutes of Health (NS-42867, RR-00165), the Kavli Institute for Brain and Mind at the University of California at San Diego, and the James S. McDonnell Foundation (22002078, 220020293).

Abbreviations

ALS	anterior limiting sulcus
AQ	asymmetry quotient
FI	frontoinsular cortex
fMRI	functional magnetic resonance imaging
ILS	inferior limiting sulcus

MRI	magnetic resonance imaging
SLS	superior limiting sulcus
VENs	von Economo neurons

References

Ackermann H, Riecker A. The contribution(s) of the insula to speech production: a review of the clinical and functional imaging literature. Brain Struct Funct. 2010; 214:419–433. [PubMed: 20512374]

Allman JM, Tetreault NA, Hakeem AY, Manaye KF, Semendeferi K, Erwin JM, Park S, Goubert V, Hof PR. The von Economo neurons in frontoinsular and anterior cingulate cortex in great apes and humans. Brain Struct Funct. 2010; 214:495–517. [PubMed: 20512377]

Amunts K, Schleicher A, Bürgel U, Mohlberg H, Uylings HB, Zilles K. Broca's region revisited: cytoarchitecture and intersubject variability. J Comp Neurol. 1999; 412:319–341. [PubMed: 10441759]

Anderson K, Bones B, Robinson B, Hass C, Lee H, Ford K, Roberts TA, Jacobs B. The morphology of supragranular pyramidal neurons in the human insular cortex: a quantitative Golgi study. Cereb Cortex. 2009; 19:2131–2144. [PubMed: 19126800]

Arnold C, Matthews LJ, Nunn CL. The 10kTrees website: a new online resource for primate phylogeny. Evol Anthropol. 2010; 19:114–118.

Barton RA. Primate brain evolution: integrating comparative, neuro-physiological, and ethological data. Evol Anthropol. 2006; 15:224–236.

Becquet C, Patterson N, Stone AC, Przeworski M, Reich D. Genetic structure of chimpanzee populations. PLoS Genet. 2007; 3:e66. [PubMed: 17447846]

Bonthius DJ, Solodkin A, Van Hoesen GW. Pathology of the insular cortex in Alzheimer disease depends on cortical architecture. J Neuropathol Exp Neurol. 2005; 64:910–922. [PubMed: 16215463]

Bush EC, Allman JM. The scaling of frontal cortex in primates and carnivores. Proc Natl Acad Sci. 2004; 101:3962–3966. [PubMed: 15007170]

Butti C, Hof PR. The insular cortex: a comparative perspective. Brain Struct Funct. 2010; 214:477–493. [PubMed: 20512368]

Butti C, Santos M, Uppal N, Hof PR. Von Economo neurons: clinical and evolutionary perspectives. Cortex. 2013; 49:312–326. [PubMed: 22130090]

Butti C, Sherwood CC, Hakeem AY, Allman JM, Hof PR. Total number and volume of von Economo neurons in the cerebral cortex of cetaceans. J Comp Neurol. 2009; 515:243–259. [PubMed: 19412956]

Cáceres M, Lachuer J, Zapala MA, Redmond JC, Kudo L, Geschwind DH, Lockhart DJ, Preuss TM, Barlow C. Elevated gene expression levels distinguish human from non-human primate brains. Proc Natl Acad Sci. 2003; 100:13030–13035. [PubMed: 14557539]

Carmichael ST, Price JL. Architectonic subdivision of the orbital and medial prefrontal cortex in the macaque monkey. J Comp Neurol. 1994; 346:366–402. [PubMed: 7527805]

Charvet, CJ.; Finlay, BL. Embracing covariation in brain evolution: large brains, extended development, and flexible primate social systems. In: Hofman, MA.; Falk, D., editors. Progress in Brain Research. Elsevier Press; Oxford: 2012. p. 71-87.

Craig AD. How do you feel? Interoception: the sense of the physiological condition of the body. Nat Rev Neurosci. 2002; 3:655–666. [PubMed: 12154366]

Craig AD. Interoception: the sense of the physiological condition of the body. Curr Opin Neurobiol. 2003; 13:500–505. [PubMed: 12965300]

Craig AD. Human feelings: why are some more aware than others? Trends Cogn Sci. 2004; 8:239–241. [PubMed: 15165543]

Craig AD. Forebrain emotional asymmetry: a neuroanatomical basis? Trends Cogn Sci. 2005; 9:566–571. [PubMed: 16275155]

Craig AD. How do you feel–now? The anterior insula and human awareness. Nat Rev Neurosci. 2009; 10:59–70. [PubMed: 19096369]

Craig AD. The sentient self. Brain Struct Funct. 2010; 214:563–577. [PubMed: 20512381]

Craig AD, Chen K, Bandy D, Reiman EM. Thermosensory activation of insula cortex. Nat Neurosci. 2000; 3:184–190. [PubMed: 10649575]

Critchley HD. Neural mechanisms of autonomic, affective, and cognitive integration. J Comp Neurol. 2005; 493:154–166. [PubMed: 16254997]

Critchley HD, Wiens S, Rotshtein P, Ohman A, Dolan RJ. Neural systems supporting interoceptive awareness. Nat Neurosci. 2004; 7:189–195. [PubMed: 14730305]

de Sousa AA, Sherwood CC, Mohlberg H, Amunts K, Schleicher A, MacLeod CE, Hof PR, Frahm H, Zilles K. Hominoid visual brain structure volumes and the position of the lunate sulcus. J Hum Evol. 2010; 58:281–292. [PubMed: 20172590]

Deacon TW. Problems of ontogeny and phylogeny in brain size evolution. Int J Primatol. 1990; 11:237–282.

Dunbar RIM. The social brain hypothesis. Evol Anthropol. 1998; 6:178–190.

Dunbar RIM, Schultz S. Evolution in the social brain. Science. 2007; 317:1344–1347. [PubMed: 17823343]

Elston GN, Benavides-Piccione R, Elston A, Zietsch B, Defelipe J, Manger P, Casagrande V, Kaas JH. Specializations of the granular prefrontal cortex of primates: Implications for cognitive processing. Anat Rec. 2006; 288:26–35.

Evrard HC, Forro T, Logothetis NK. Von Economo neurons in the anterior insula of the macaque monkey. Neuron. 2012; 74:482–489. [PubMed: 22578500]

Evrard, HC.; Zilles, K.; Sherwood, CC.; Logothetis, NK. Program No. 817.15. 2011 Neuroscience Meeting Planner. Society for Neuroscience; Washington, DC: 2011. Large spindle-shaped neurons in the anterior insula in lesser apes and monkeys. (Online)

Fajardo C, Escobar MI, Buriticá E, Arteaga G, Umbarila J, Casanova MF, Pimienta H. Von Economo neurons are present in the dorsolateral (dysgranular) prefrontal cortex of humans. Neurosci Lett. 2008; 435:215–218. [PubMed: 18355958]

Forro, T.; Logothetis, NK.; Evrard, HC. Abstract No. 817.07. 2011 Neuroscience Meeting Planner. Society for Neuroscience; Washington, DC: 2011. Distribution of a large spindle-shaped neuron in the anterior agranular insula in the macaque monkey.

Freckleton RP, Harvey PH, Pagel M. Phylogenetic analysis and comparative data: a test and review of evidence. Am Nat. 2002; 160:712–726. [PubMed: 18707460]

Galaburda AM, Sanides F. Cytoarchitectonic organization of the human auditory cortex. J Comp Neurol. 1980; 190:597–610. [PubMed: 6771305]

Gallay DS, Gallay MN, Jeanmonod D, Rouiller EM, Morel A. The insula of Reil revisited: multiarchitectonic organization in macaque monkeys. Cereb Cortex. 2011; 22:175–190. [PubMed: 21613468]

Glezer II. Area relationships in the precentral region in a comparative-anatomical series of primates. Arkhiv Anat Gistol Embriol. 1958; 2:26.

Goodman M, Tagle DA, Fitch DH, Bailey W, Czelusniak J, Koop BF, Benson P, Slightom JL. Primate evolution at the DNA level and a classification of hominoids. J Mol Evol. 1990; 30:260–266. [PubMed: 2109087]

Hakeem AY, Sherwood CC, Bonar CJ, Butti C, Hof PR, Allman JM. Von Economo neurons in the elephant brain. Anat Rec. 2009; 292:242–248.

Harvey PH, Krebs JR. Comparing brains. Science. 1990; 249:140–146. [PubMed: 2196673]

Hey J. The divergence of chimpanzee species and subspecies as revealed in multipopulation isolation-with-migration analyses. Mol Biol Evol. 2010; 27:921–933. [PubMed: 19955478]

Hof PR, Van der Gucht E. The structure of the cerebral cortex of the humpback whale, *Megaptera novaeangliae* (Cetacea, Mysticeti, Balaenopteridae). Anat Rec. 2007; 290:1–31.

Holloway RL. Within-species brain-body weight variability: a reexamination of the Danish data and other primate species. Am J Phys Anthrop. 1980; 53:109–121. [PubMed: 7416241]

Holloway, RL. Toward a synthetic theory of human brain evolution. In: Changeux, JP.; Chavaillon, J., editors. Origins of the Human Brain. Clarendon Press; Oxford: 1996. p. 42-54.

Jacobs B, Schall M, Prather M, Kapler E, Driscoll L, Baca S, Jacobs J, Ford K, Wainwright M, Treml M. Regional dendritic and spine variation in human cerebral cortex: a quantitative Golgi study. Cereb Cortex. 2001; 11:558–571. [PubMed: 11375917]

Jerison, HJ. Evolution of the Brain and Intelligence. Academic Press; New York: 1973.

Kaas JH. Why is brain size so important: design problems and solutions as neocortex gets bigger and smaller. Mind Brain. 2000; 1:7–23.

Kaufman JA, Paul LK, Manaye KF, Granstedt AE, Hof PR, Hakeem AY, Allman JM. Selective reduction of Von Economo neuron number in agenesis of the corpus callosum. Acta Neuropathol. 2008; 116:479–489. [PubMed: 18815797]

Kim EJ, Sidhu M, Gaus SE, Huang EJ, Hof PR, Miller BL, Dearmond SJ, Seeley WW. Selective frontoinsular von Economo neuron and fork cell loss in early behavioral variant frontotemporal dementia. Cereb Cortex. 2012; 22:251–259. [PubMed: 21653702]

Kurth F, Eickhoff SB, Schleicher A, Hoemke L, Zilles K, Amunts K. Cytoarchitecture and probabilistic maps of the human posterior insular cortex. Cereb Cortex. 2010a; 20:1448–1461. [PubMed: 19822572]

Kurth F, Zilles K, Fox PT, Laird AR, Eickhoff SB. A link between the systems: functional differentiation and integration within the human insula revealed by meta-analysis. Brain Struct Funct. 2010b; 214:519–534. [PubMed: 20512376]

Lamm C, Singer T. The role of anterior insular cortex in social emotions. Brain Struct Funct. 2010; 214:579–591. [PubMed: 20428887]

MacNeilage PF, Rogers LJ, Vallortigara G. Origins of the left and right brain. Sci Am. 2009; 301:60–67. [PubMed: 19555025]

Martins EP, Diniz-Filho JAF, Housworth EA. Adaptive constraints and the phylogenetic comparative method: a computer simulation test. Evolution. 2002; 56:1–13. [PubMed: 11913655]

Martins EP, Hansen TF. Phylogenies and the comparative method: a general approach to incorporating phylogenetic information into the analysis of inter-specific data. Am Nat. 1997; 149:646–667.

Mesulam MM, Mufson EJ. Insula of the Old World monkey. I: architectonics in the insulo-orbito-temporal component of the paralimbic brain. J Comp Neurol. 1982; 212:1–22. [PubMed: 7174905]

Mitani JC, Watts DP, Amsler SJ. Lethal intergroup aggression leads to territorial expansion in wild chimpanzees. Curr Biol. 2010; 20:R507–R508. [PubMed: 20620900]

Mutschler I, Wieckhorst B, Kowalevski S, Derix J, Wentlandt J, Schulze-Bonhage A, Ball T. Functional organization of the human anterior insular cortex. Neurosci Lett. 2009; 457:66–70. [PubMed: 19429164]

Naidich TP, Kang E, Fatterpekar GM, Delman BN, Gultekin SH, Wolfe D, Ortiz O, Yousry I, Weismann M, Yousry TA. The insula: anatomic study and MR imaging display at 1.5 T. Am J Neuroradiol. 2004; 25:222–232. [PubMed: 14970021]

Nieuwenhuys, R. The insular cortex: a review. In: Hofman, MA.; Falk, D., editors. Progress in Brain Research. Elsevier Press; Oxford: 2012. p. 123-163.

Nimchinsky EA, Gilissen E, Allman JM, Perl DP, Erwin JM, Hof PR. A neuronal morphologic type unique to humans and great apes. Proc Natl Acad Sci. 1999; 96:5268–5273. [PubMed: 10220455]

Nimchinsky EA, Vogt BA, Morrison JH, Hof PR. Spindle neurons of the human anterior cingulate cortex. J Comp Neurol. 1995; 355:27–37. [PubMed: 7636011]

Nunn CL. Spleen size, disease risk and sexual selection: a comparative study in primates. Evol Ecol Res. 2002; 4:91–107.

Nunn, CL.; van Schaik, CP. A comparative approach to reconstructing the socioecology of extinct primates. In: Plavcan, JM., editor. Reconstructing Behavior in the Primate Fossil Record. Kluwer Academic/Plenum; New York: 2001. p. 159-216.

Öngür D, Ferry AT, Price JL. Architectonic subdivision of the human orbital and medial prefrontal cortex. J Comp Neurol. 2003; 460:425–449. [PubMed: 12692859]

O'Neill MC, Dobson SD. The degree and pattern of phylogenetic signal in primate long-bone structure. J Hum Evol. 2008; 54:309–322. [PubMed: 17931688]

Ostrowsky K, Magnin M, Ryvlin P, Isnard J, Guenot M, Mauguière F. Representation of pain and somatic sensation in the human insula: a study of responses to direct electrical cortical stimulation. Cereb Cortex. 2002; 12:376–385. [PubMed: 11884353]

Pagel M. Inferring the historical patterns of biological evolution. Nature. 1999; 401:877–884. [PubMed: 10553904]

Pagel M, Meade A, Barker D. Bayesian estimation of ancestral character states on phylogenies. Syst Biol. 2004; 53:673–684. [PubMed: 15545248]

Preuss, TM. What's human about the human brain?. In: Gazzaniga, MS., editor. The New Cognitive Neurosciences. 2. MIT Press; Cambridge: 2000. p. 1219-1234.

Preuss TM, Cáceres M, Oldham MC, Geschwind DH. Human brain evolution: insights from microarrays. Nat Rev Genet. 2004; 5:850–860. [PubMed: 15520794]

Preuss TM, Goldman-Rakic PS. Myelo- and cytoarchitecture of the granular frontal cortex and surrounding regions in the strepsirhine primate *Galago* and the anthropoid primate *Macaca*. J Comp Neurol. 1991; 310:429–474. [PubMed: 1939732]

Price JL. Prefrontal cortical networks related to visceral function and mood. Ann NY Acad Sci. 1999; 877:383–396. [PubMed: 10415660]

Revell LJ. Phylogenetic signal and linear regression on species data. Methods Ecol Evol. 2010; 1:319–329.

Rilling JK, Goldsmith DR, Glenn AL, Jairam MR, Elfenbein HA, Dagenais JE, Murdock CD, Pagnoni G. Neural correlates of the affective response to unreciprocated cooperation. Neuropsychologia. 2008; 46:1256–1266. [PubMed: 18206189]

Rilling JK, Insel TR. The primate neocortex in comparative perspective using magnetic resonance imaging. J Hum Evol. 1999; 37:191–223. [PubMed: 10444351]

Rilling JK, Sanfey AG. The neuroscience of social decision-making. A Rev Psychol. 2011; 62:23–48.

Rilling JK, Scholz J, Preuss TM, Glasser MF, Errangi BK, Behrens TE. Differences between chimpanzees and bonobos in neural systems supporting social cognition. Soc Cogn Affect Neurosci. 2011; 7:369–379. [PubMed: 21467047]

Rose M. Die Inselrinde des Menschen und der Tiere. J Psychol Neurol. 1928; 37:467–624.

Russo D, Paparcone R, Genovese A. A cytoarchitectonic and myeloarchitectonic study of the insular cortex of the bull, *Bos taurus*. Acta Histochem. 2008; 110:245–255. [PubMed: 18160101]

Santos M, Uppal N, Butti C, Wicinski B, Schmeidler J, Giannakopoulos P, Heinsen H, Schmitz C, Hof PR. Von Economo neurons in autism: a stereologic study of the frontoinsular cortex in children. Brain Res. 2011; 138:206–217. [PubMed: 20801106]

Schenker NM, Hopkins WD, Spocter MA, Garrison AR, Stimpson CD, Erwin JM, Hof PR, Sherwood CC. Broca's area homologue in chimpanzees (*Pan troglodytes*): probabilistic mapping, asymmetry, and comparison to humans. Cereb Cortex. 2010; 20:730–742. [PubMed: 19620620]

Schleicher A, Palomero-Gallagher N, Morosan P, Eickhoff SB, Kowalski T, de Vos K, Amunts K, Zilles K. Quantitative architectural analysis: a new approach to cortical mapping. Anat Embryol (Berl). 2005; 210:373–386. [PubMed: 16249867]

Seeley WW, Carlin DA, Allman JM, Macedo MN, Bush C, Miller BL, DeArmond SJ. Early frontotemporal dementia targets neurons unique to apes and humans. Ann Neurol. 2006; 60:660–667. [PubMed: 17187353]

Semendeferi K, Armstrong E, Schleicher A, Zilles K, Van Hoesen GW. Limbic frontal cortex in hominoids: a comparative study of area 13. Am J Phys Anthropol. 1998; 106:129–155. [PubMed: 9637180]

Semendeferi K, Armstrong E, Schleicher A, Zilles K, Van Hoesen GW. Prefrontal cortex in humans and apes: a comparative study of area 10. Am J Phys Anthropol. 2001; 114:224–241. [PubMed: 11241188]

Semendeferi K, Damasio H. The brain and its main anatomical subdivisions in living hominoids using magnetic resonance imaging. J Hum Evol. 2000; 38:317–332. [PubMed: 10656781]

Semendeferi K, Teffer K, Buxhoeveden DP, Park MS, Bludau S, Amunts K, Travis K, Buckwalter J. Spatial organization of neurons in the frontal pole sets humans apart from great apes. Cereb Cortex. 2010; 21:1485–1497. [PubMed: 21098620]

Silk JB, House BR. Evolutionary foundations of human prosocial sentiments. Proc Natl Acad Sci. 2011; 108:10910–10917. [PubMed: 21690372]

Singer T, Critchley HD, Preuschoff K. A common role of insula in feelings, empathy and uncertainty. Trends Cogn Sci. 2009; 13:334–340. [PubMed: 19643659]

Singer T, Seymour B, O'Doherty J, Kaube H, Dolan RJ, Frith CD. Empathy for pain involves the affective but not sensory components of pain. Science. 2004; 303:1157–1162. [PubMed: 14976305]

Singer T, Seymour B, O'Doherty JP, Stephan KE, Dolan RJ, Frith CD. Empathic neural responses are modulated by the perceived fairness of others. Nature. 2006; 439:466–469. [PubMed: 16421576]

Smaers JB, Schleicher A, Zilles K, Vinicius L. Frontal white matter volume is associated with brain enlargement and higher structural connectivity in anthropoid primates. PLoS One. 2010; 5:e9123. [PubMed: 20161758]

Smaers JB, Steele J, Case CR, Cowper A, Amunts K, Zilles K. Primate prefrontal cortex evolution: human brains are the extreme of a lateralized ape trend. Brain Behav Evol. 2011; 77:67–78. [PubMed: 21335939]

Smith RJ. Logarithmic transformation bias in allometry. Am J Phys Anthropol. 1993; 90:215–228.

Smith RJ. Use and misuse of the reduced major axis for line-fitting. Am J Phys Anthropol. 2009; 140:476–486. [PubMed: 19425097]

Smith RJ, Jungers WL. Body mass in comparative primatology. J Hum Evol. 1997; 32:523–559. [PubMed: 9210017]

Sokal, RR.; Rohlf, FJ. Biometry: The Principles and Practice of Statistics in Biological Research. 3. W.H. Freeman; New York: 1995.

Spocter MA, Hopkins WD, Garrison AR, Bauernfeind AL, Stimpson CD, Hof PR, Sherwood CC. Wernicke's area homologue in chimpanzees (*Pan troglodytes*) and its relation to the appearance of modern human language. Proc R Soc B. 2010; 277:2165–2174.

Stephan H. Methodische Studien über den quantitativen Vergleich architektonischer Struktureinheiten des Gehirns. Z Wiss Zool. 1960; 164:143–172.

Striedter, G. Principles of Brain Evolution. Sinauer Associates; Sunderland: 2005.

Townsend SW, Slocombe KE, Thompson ME, Zuberbühler K. Female-led infanticide in wild chimpanzees. Curr Biol. 2007; 17:R355–R356. [PubMed: 17502085]

Türe U, Yaşargil DC, Al-Mefty O, Yaşargil MG. Topographic anatomy of the insular region. J Neurosurg. 1999; 90:720–733. [PubMed: 10193618]

Uddin M, Wildman DE, Liu G, Xu W, Johnson RM, Hof PR, Kapatos G, Grossman LI, Goodman M. Sister grouping of chimpanzees and humans as revealed by genome-wide phylogenetic analysis of brain gene expression profiles. Proc Natl Acad Sci. 2004; 101:2957–2962. [PubMed: 14976249]

von Economo C. Eine neue Art Spezialzellen des Lobus cinguli und Lobus insulae. Zschr Ges Neurol Psychiat. 1926; 100:706–712.

Wager, TD.; Barrett, LF. From Affect to Control: Functional Specialization of the Insula in Motivation and Regulation. 2004. Available from: PsycExtra,. http://www.columbia.edu/cu/psychology/tor/

Watkins KE, Paus T, Lerch JP, Zijdenbos A, Collins DL, Neelin P, Taylor J, Worsley KJ, Evans AC. Structural asymmetries in the human brain: a voxel-based statistical analysis of 142 MRI scans. Cereb Cortex. 2001; 11:868–877. [PubMed: 11532891]

Wrangham RW, Wilson ML, Muller MN. Comparative rates of violence in chimpanzees and humans. Primates. 2006; 47:14–26. [PubMed: 16132168]

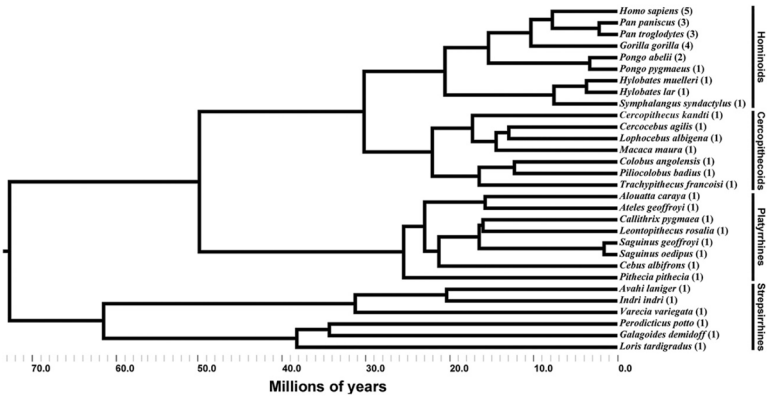

Figure 1.

Phylogenetic tree of primates included in this study. The length of each branch represents the distance in evolutionary time. The number in parentheses represents the number of individuals of that species sampled.

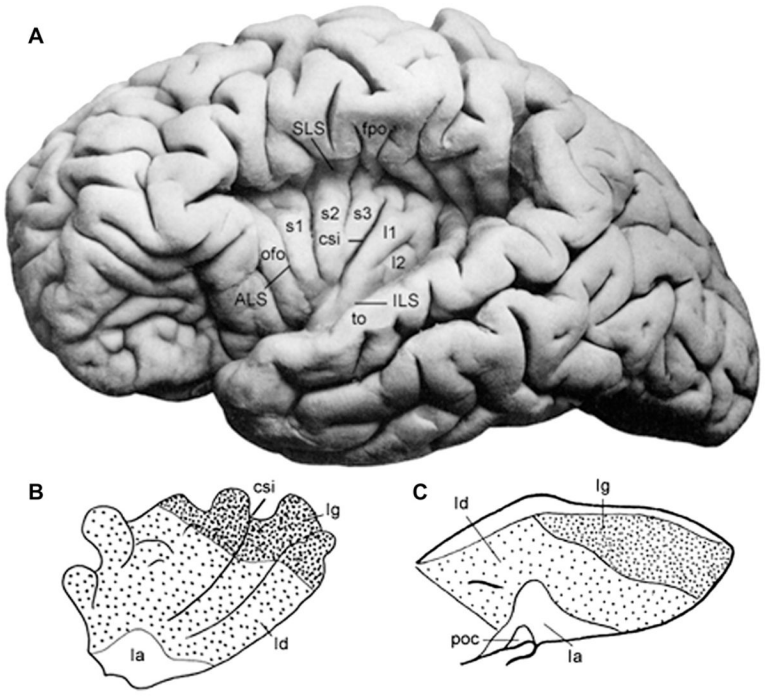

Figure 2.

Lateral views of insular cortex. In (A), the left insula of a human has been exposed by removing the overlying opercula. (B) and (C) are schematics displaying the cytoarchitecture of the insulae in *Homo sapiens* and *Macaca mulatta*, respectively. In both images, the insulae are parcellated into granular (Ig), dysgranular (Id), and agranular (Ia) regions. The relative positions of these subdivisions of insular cortex are similar in both species. The central sulcus of the insula (csi) is labeled in the human. Other notations: Anterior limiting sulcus (ALS); first (s1), second (s2), and third short gyri (s3); first (l1) and second long gyri (l2); inferior limiting sulcus (ILS); orbitofrontal operculum (ofo); frontoparietal operculum (fpo); temporal operculum (to); piriform olfactory cortex (poc); superior limiting sulcus (SLS). (A), (B), and (C) are modified from Nieuwenhuys (2012). All figures are oriented so the anterior surface is on the left. The figures are not to scale.

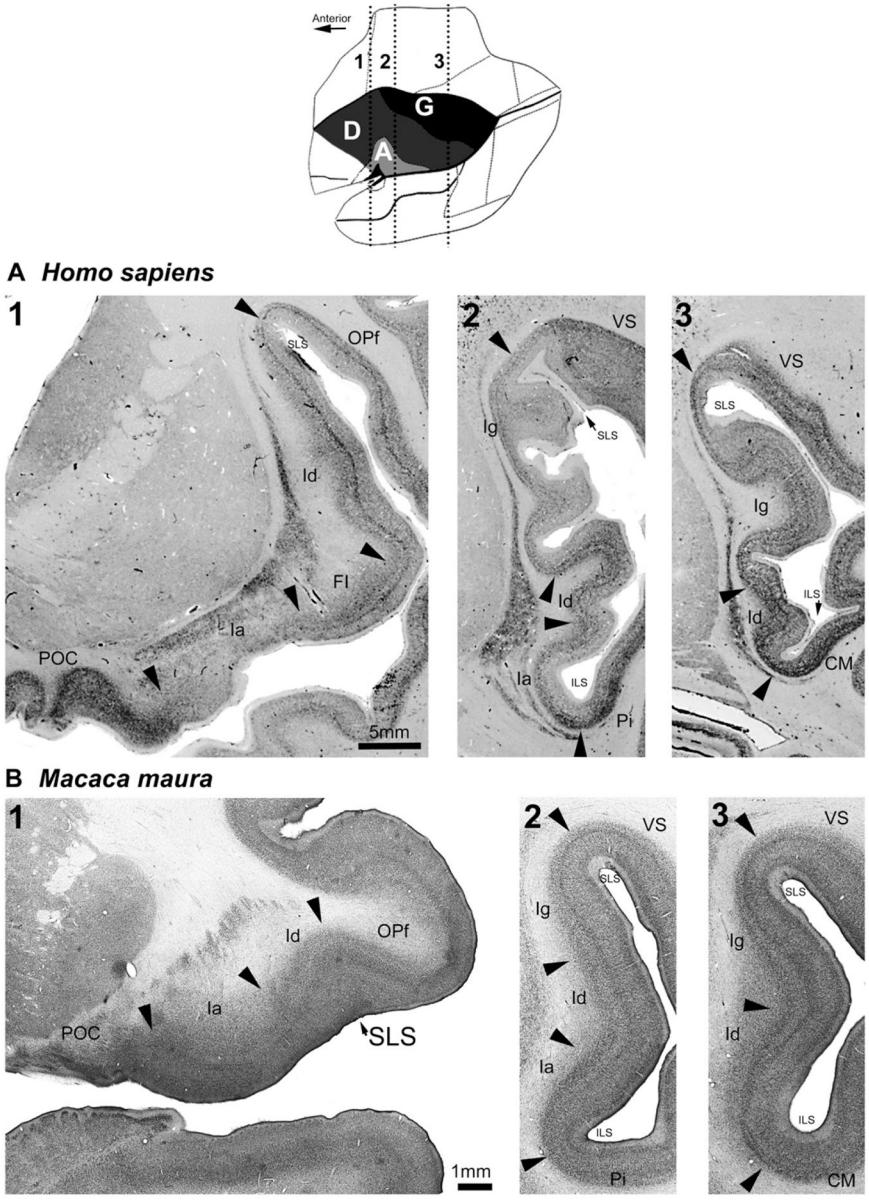

Figure 3.

Nissl-stained coronal sections of insular cortex in (A) *Homo sapiens* and (B) *Macaca maura*. Human sections were taken from the online resources of the human brain Atlas at Michigan state University (https://www.msu.edu/~brains/brains/human/index.html). Macaque sections were photographed from the GAAP collection. The scale is the same for all sections within a species. The schematic at the top of the figure is a modified diagram of *Macaca mulatta* from Mesulam and Mufson (1982) to show the approximate anterior–posterior plane of each of the coronal sections, which are labeled by numbers. Arrows mark the transitions between cortical areas. The abbreviations are the same as in Figure 1. SLS and ILS refer to the superior and inferior limbs of the Sylvian fissure, respectively. In *H. sapiens*, FI is labeled. Other notations: caudomedial area of the auditory belt (CM), agranular insula (Ia), dysgranular insula (Id), granular insula (Ig), frontal opercular area (OPf), parainsular area

(Pi), piriform olfactory cortex (POC), and ventral somatosensory area (VS). All images of a species share the scale indicated in the leftmost image.

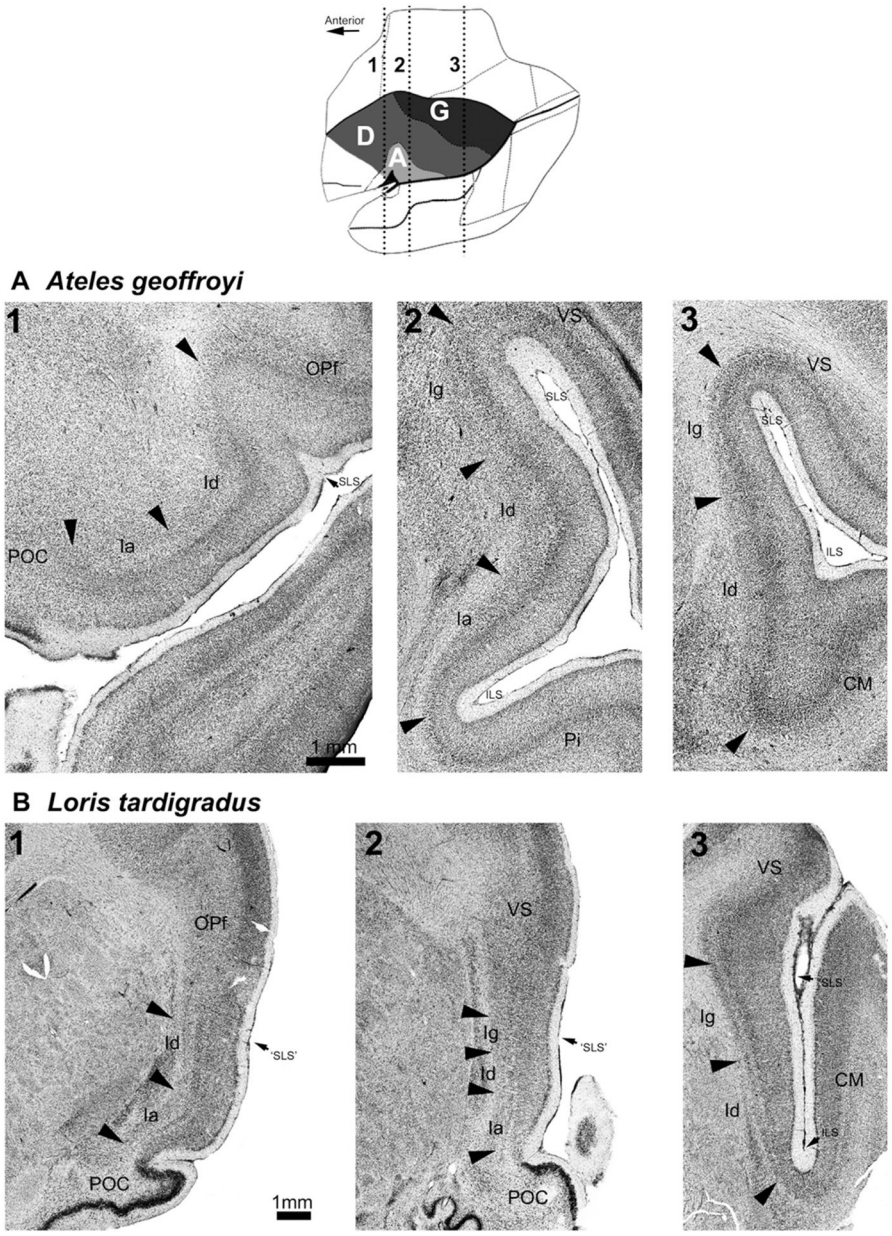

Figure 4.

Nissl-stained coronal sections of insular cortex in (A) *Ateles geoffroyi* and (B) *Loris tardigradus*. Sections from both species were photographed from the GAAP collection. The scale is the same for all sections within a species. The schematic at the top of the figure is a modified diagram of *Macaca mulatta* from Mesulam and Mufson (1982) to show the approximate anterior–posterior plane of each of the coronal sections, which are labeled with numbers. Arrows mark the transitions between cortical areas. The abbreviations are the same as those used in Figure 3. 'SLS' in the coronal series from the *Loris* refers to the bend in the cortical tissue that is homologous to the SLS. All images of a species share the scale indicated in the leftmost image.

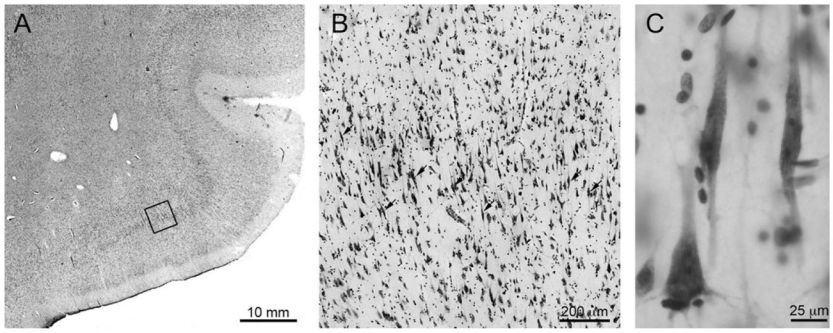

Figure 5.
Nissl-stained FI and VENs in the anterior insula of a human. The boxed region in A is magnified in B. C displays VENs under high magnification. FI is agranular insular cortex (A) that contains clusters of VENs in layer Vb. In humans and great apes, VENs (marked by arrows in B) are found in the highest density on or near the crowns of gyri. VENs are cells with a bipolar morphology (C). The cell in the lower left corner of C is a pyramidal neuron. Photomicrographs B and C are oriented with the pial surface at the top of the image.

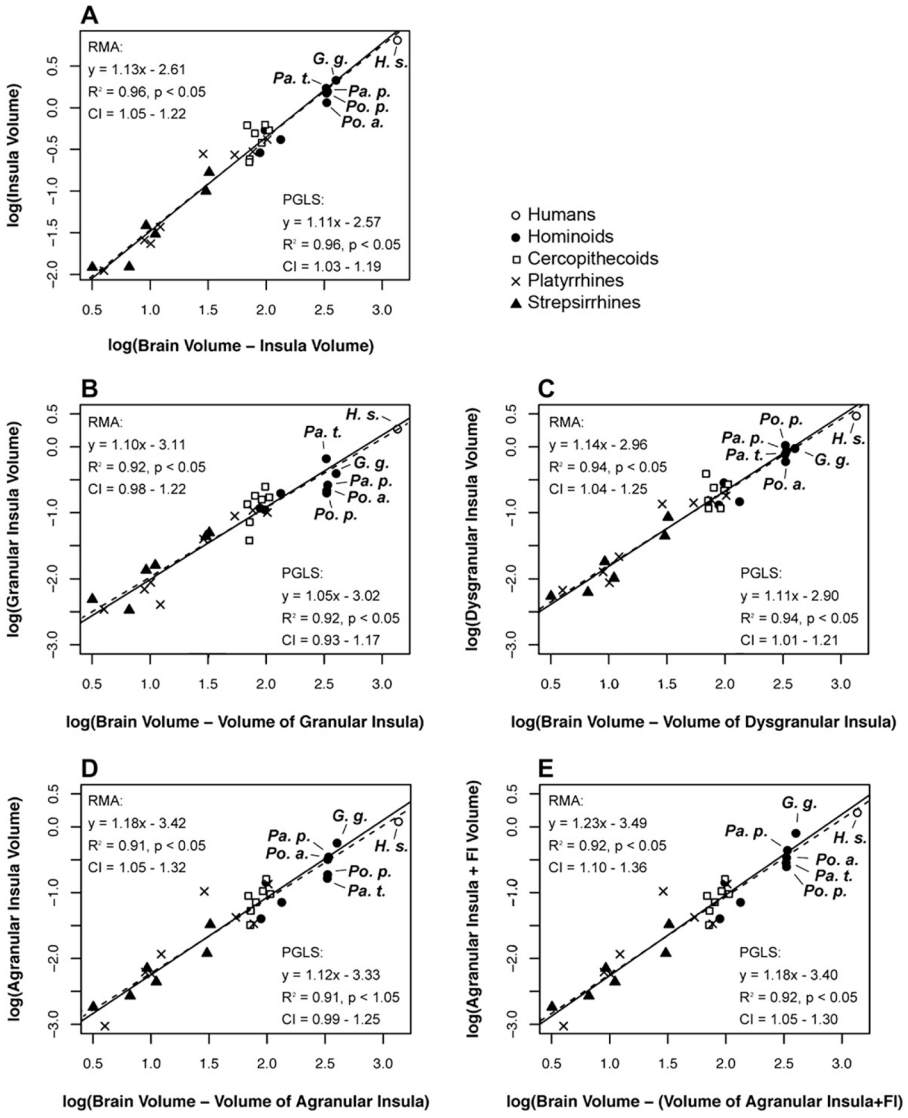

Figure 6.

Linear regressions of the total insula volume (A) and the volume of its subdivisions (B–E) in the left hemisphere against total brain volume. Results of both RMA (solid lines) and PGLS (dashed lines) analyses are shown. Because the VEN-containing portion of agranular insula in great apes and humans is referred to as FI in this study, agranular insula and FI are combined (6E) for agranular insula to be compared in all primate taxa included. Individual hominoid species are labeled with abbreviations of their scientific names (*H. s.* = *Homo sapiens*, *Pa. t.* = *Pan troglodytes*, *Pa. p.* = *Pan paniscus*, *Po. p.* = *Pongo pygmaeus*, *Po. a.* = *Pongo abelii*).

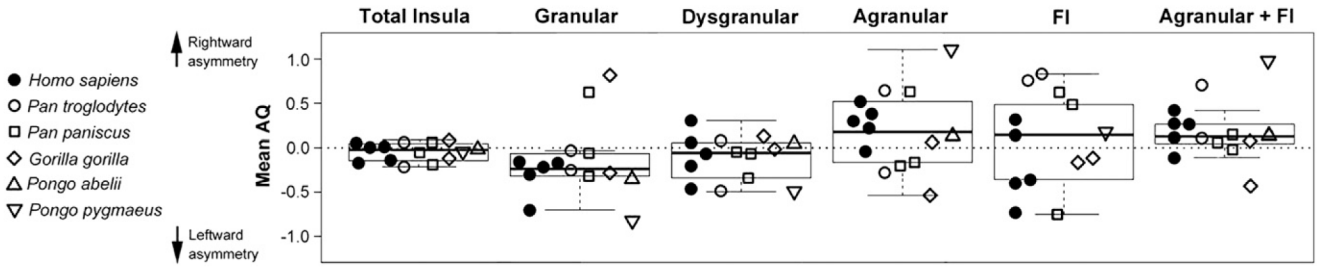

Figure 7.

Asymmetry quotient (AQ) values for the insula as a whole and each of its cytoarchitectural subdivisions. Each specimen, in which volume estimates could be obtained for the left and right insulae and its cytoarchitectural subdivisions, is represented by its own symbol. Each symbol represents a single species. The whiskers extend to the largest/smallest observations within a distance of 1.5 times the interquartile range.

Table 1

List of individuals and stereologic estimates of shrinkage-corrected volumes for left insula and its subdivisions. Body mass estimates (Smith and Jungers,1997) and population group sizes (Nunn and van Schaik, 2001; Nunn, 2002) were collected from previously published literature. *Pongo abelii*, *Cercocebus agilis*, and *Cercopithecus kandti* are not included in the phylogenetic analysis because group size estimates were not found.

Volume estimates of left insular subdivisions (cm^3)														
Species	**Individual**	**Collection**	**Section thickness (mm)**	**Age**	**Sex**	**Body mass estimates (kg)**	**Social group size**	**Brain mass (g)**	**Brain volume (cm^3)**	**Granular**	**Dysgranular**	**Agranular**	**FI**	**Total insula volume**
Homo sapiens	H9-88[a]	UCSD	35	21	Male	72.1	148	1639.6	1582.6	2.356	3.321	1.518	0.539	7.734
H. sapiens	MU-88-65[a]	Yakovlev-Haleem	35	50	Male	72.1	148	1483.0	1431.5	1.410	2.709	1.781	0.562	6.463
H. sapiens	SN207-84[a]	UCSD	35	75	Male	72.1	148	1349.0	1302.1	2.246	2.971	1.342	0.349	6.908
H. sapiens	W2-2-70[a]	Yakovlev-Haleem	35	25	Male	72.1	148	1320.0	1274.1	1.959	3.850	0.973	0.442	7.222
H. sapiens	STD-IIA-54[a]	Yakovlev-Haleem	35	32	Female	62.1	148	1242.0	1198.8	1.398	1.950	0.389	0.331	4.068
Pan paniscus	Nambo[b]	GAAP	100	–	Male	45	43.4	395.0	381.27	0.167	0.771	0.484	0.121	1.543
P. paniscus	MCZ-2007-52[a]	GAAP	40	25	Female	33.2	43.4	337.0	325.29	0.267	1.067	0.356	0.086	1.775
P. paniscus	Zahlia[a]	UCSD	20	11	Female	33.2	43.4	324.0	312.74	0.348	0.965	0.213	0.227	1.753
Pan troglodytes	CA0171[b]	GAAP	100	39	Male	49.57	47.6	374.0	361	0.357	0.753	0.211	0.066	1.387
P. troglodytes	YN01-92[a]	GAAP	40	40	Male	49.57	47.6	341.2	329.34	0.886	0.757	0.203	0.097	1.942
P. troglodytes	YN00-170[a]	GAAP	40	45	Female	40.37	47.6	312.9	302.03	0.759	0.601	0.080	0.034	1.473
Gorilla gorilla	OON1072[b]	GAAP	100	25	Male	169.37	15.8	450.0	434.36	0.642	0.793	0.554	0.522	2.510
G. gorilla	862094[b]	GAAP	100	39	Female	80	15.8	420.0	405.41	0.466	0.875	0.479	0.161	1.982
G. gorilla	439[b]	GAAP	100	33	Female	80	15.8	419.0	404.44	0.348	1.170	0.496	0.166	2.180
G. gorilla	YN82-140[a]	UCSD	20	20	Female	80	15.8	376.0	362.93	0.122	0.957	0.751	0.079	1.910
Pongo abelii	M00305[b]	GAAP	100	17	Female	35.6	–	358.0	345.56	0.266	0.622	0.317	0.000	1.204
P. abelii	Thelma[b]	GAAP	100	25	Female	35.6	–	333.8	322.2	0.171	0.577	0.326	0.039	1.112
Pongo pygmaeus	Sabtu[b,c]	GAAP	100	39	Female	35.6	1.5	376.0	362.93	–	–	–	–	–
P. pygmaeus	Briggs[a]	UCSD	20	34	Male	78.5	1.5	345.0	333.01	0.199	1.057	0.188	0.060	1.505
Hylobates muelleri	970431[a]	GAAP	40	19	Male	5.71	3.4	101.8	98.263	0.111	0.286	0.142	–	0.539
Hylobates lar	YN81-146[b]	Stephan	20	–	Female	5.34	3.8	92.0	88.803	0.117	0.131	0.040	–	0.289

Volume estimates of left insular subdivisions (cm^3)

Species	Individual	Collection	Section thickness (mm)	Age	Sex	Body mass estimates (kg)	Social group size	Brain mass (g)	Brain volume (cm^3)	Granular	Dysgranular	Agranular	FI	Total insula volume
Symphalangus syndactylus	880804[a]	GAAP	40	33	Male	11.9	4	138.7	133.88	0.198	0.147	0.071	–	0.416
Cercopithecus kandti	201202[a]	GAAP	40	–	Male	5.48	–	71.6	69.112	0.134	0.391	0.089	–	0.614
Cercocebus agilis	980820[a]	GAAP	40	19	Female	5.66	–	95.3	91.988	0.158	0.116	0.105	–	0.379
Lophocebus albigena	3407[b]	Stephan	20	–	Male	8.25	15.5	110.5	106.66	0.171	0.270	0.095	–	0.536
Macaca maura	M1005[a]	GAAP	40	5	Female	6.05	22	83.3	80.405	0.181	0.240	0.071	–	0.492
Colobus angolensis	M00652[a]	GAAP	40	18	Male	9.68	8.8	74.4	71.815	0.038	0.152	0.032	–	0.222
Piliocolobus badius	3477[b]	Stephan	15	–	Female	7.05	30.2	75.0	72.394	0.072	0.116	0.053	–	0.241
Trachypithecus francoisi	51106[a]	GAAP	40	16	Male	7.7	17.1	102.1	98.552	0.249	0.217	0.160	–	0.625
Alouatta caraya	890708[a]	GAAP	40	21	Male	6.42	7.9	55.8	53.861	0.089	0.141	0.042	–	0.272
Ateles geoffroyi	3371[b]	Stephan	20	–	Male	7.78	22.7	106.4	102.7	0.100	0.181	0.135	–	0.416
Callithrix pygmaea	3289[b]	Stephan	20	–	Male	0.11	7.9	4.2	4.0058	0.003	0.007	0.001	–	0.011
Leontopithecus rosalia	950728[a]	GAAP	40	11	Female	0.598	4.5	12.7	12.259	0.004	0.021	0.012	–	0.037
Saguinus geoffroyi	900722[a]	GAAP	40	15	Male	0.482	5.2	10.5	10.135	0.009	0.009	0.006	–	0.023
Saguinus oedipus	3311[b]	Stephan	20	–	Male	0.418	5.3	9.3	8.9382	0.007	0.013	0.006	–	0.026
Cebus albifrons	3317[b]	Stephan	20	–	Male	3.18	19.2	79.8	77.027	0.108	0.155	0.034	–	0.297
Pithecia pithecia	M30709[a]	GAAP	40	1	Female	1.58	2.6	30.0	28.958	0.040	0.135	0.104	–	0.279
Avahi laniger	3244[b]	Stephan	15	–	Male	1.03	2.5	9.6	9.2568	0.013	0.018	0.007	–	0.038
Indri indri	3249[b]	Stephan	15	–	Male	5.83	4.3	33.7	32.481	0.050	0.085	0.033	–	0.167
Varecia variegata	3227[b]	Stephan	15	–	Male	3.55	5.4	31.5	30.405	0.044	0.044	0.012	–	0.100
Perodicticus potto	3259[b]	Stephan	20	–	Male	1.25	1	11.5	11.1	0.016	0.010	0.004	–	0.031
Galagoides demidoff	3275[b]	Stephan	20	–	Male	0.063	3.5	3.3	3.1853	0.005	0.005	0.002	–	0.012
Loris tardigradus	3253[b]	Stephan	20	–	Male	0.264	3	6.9	6.612	0.003	0.006	0.003	–	0.012

[a]Volumes estimated using StereoInvestigator software.

[b]Volumes estimated using ImageJ software.

[c]The left hemisphere was unavailable.

Table 2

Stereologic estimates of shrinkage-corrected volumes (cm^3) for right insula and its subdivisions in each human and great ape sampled.

Volume estimates of right insular subdivisions (cm^3)						
Species	**Individual**	**Granular**	**Dysgranular**	**Agranular**	**FI**	**Total insula volume**
Homo sapiens	H9-88	1.984	3.509	2.062	0.253	7.809
H. sapiens	MU-88-65	1.136	2.208	1.710	0.391	5.445
H. sapiens	SN207-84	1.914	1.860	1.973	0.233	5.980
H. sapiens	W2-2-70	1.456	3.638	1.653	0.509	7.255
H. sapiens	STD-IIA-54	0.673	2.650	0.485	0.454	4.262
Pan paniscus	Nambo	0.310	0.728	0.394	0.199	1.631
P. paniscus	MCZ-2007-52	0.250	0.756	0.302	0.163	1.470
P. paniscus	Zahlia	0.252	0.902	0.408	0.103	1.665
Pan troglodytes	CA0171	0.346	0.816	0.160	0.146	1.468
P. troglodytes	YN00-170	0.585	0.366	0.155	0.082	1.188
Gorilla gorilla	862094	0.349	0.996	0.276	0.136	1.757
G. gorilla	YN82-140	0.282	0.933	0.798	0.071	2.084
Pongo abelii	M00305	0.186	0.652	0.361	0.000	1.199
Pongo pygmaeus	Sabtu	0.313	0.997	0.474	0.000	1.784
P. pygmaeus	Briggs	0.083	0.637	0.654	0.072	1.446

Table 3

Species averages of volumes (cm^3) for right and left insular cortex in great apes and humans.

		Volume estimates of left insular subdivisions (cm^3)						Volume estimates of right insular subdivisions (cm^3)				
Species	***n***	**Granular**	**Dysgranular**	**Agranular**	**FI**	**Total**	***n***	**Granular**	**Dysgranular**	**Agranular**	**FI**	**Total**
Homo sapiens	5	1.87 ± 0.45	2.96 ± 0.71	1.20 ± 0.54	0.44 ± 0.11	6.48 ± 1.43	5	1.43 ± 0.55	2.77 ± 0.78	1.58 ± 0.63	0.37 ± 0.12	6.15 ± 1.42
Pan paniscus	3	0.26 ± 0.09	0.93 ± 0.15	0.35 ± 0.14	0.14 ± 0.07	1.69 ± 0.13	3	0.27 ± 0.03	0.80 ± 0.09	0.37 ± 0.06	0.16 ± 0.05	1.59 ± 0.10
Pan troglodytes	3	0.67 ± 0.28	0.70 ± 0.09	0.16 ± 0.07	0.07 ± 0.03	1.60 ± 0.30	2	0.47 ± 0.17	0.59 ± 0.32	0.16 ± 0.00	0.11 ± 0.04	1.33 ± 0.20
Gorilla gorilla	4	0.39 ± 0.22	0.95 ± 0.16	0.57 ± 0.12	0.23 ± 0.20	2.15 ± 0.27	2	0.32 ± 0.05	0.96 ± 0.04	0.54 ± 0.37	0.10 ± 0.05	1.92 ± 0.23
Pongo abelii	2	0.22 ± 0.07	0.60 ± 0.03	0.32 ± 0.01	0.02 ± 0.02	1.16 ± 0.07	1	0.186	0.652	0.361	0.000	1.199
Pongo pygmaeus	1	0.199	1.057	0.188	0.060	1.505	2	0.20 ± 0.16	0.82 ± 0.25	0.56 ± 0.12	0.04 ± 0.05	1.61 ± 0.24

Table 4

Results of the linear regressions of each region of insular cortex against estimated body mass.

	RMA results			PGLS results		
	b	**95% CI**	R^2	***b***	**95% CI**	R^2
Brain volume vs. Body mass	0.78	0.69–0.89	0.92	0.31	0.27–0.36	0.89
Insula vs. Body mass	0.78	0.69–0.89	0.92	0.37	0.32–0.42	0.91
Granular insula vs. Body mass	0.84	0.71–0.99	0.86	0.33	0.28–0.40	0.86
Dysgranular insula vs. Body mass	0.90	0.77–1.05	0.89	0.36	0.30–0.42	0.87
Agranular insula vs. Body mass	0.94	0.80–1.10	0.88	0.38	0.32–0.44	0.88
Agranular insula + FI vs. Body mass	0.99	0.85–1.15	0.89	0.38	0.32–0.44	0.87

Table 5

Percent differences between the observed volume of left insular cortex and its subdivisions in humans and the predicted volumes of these regions based on LS scaling of nonhuman primates. Within each region, human values fall within the 95% confidence intervals of nonhuman primates.

			Observed/Predicted × 100%				
Individual	**Age**	**Sex**	**Granular**	**Dysgranular**	**Agranular**	**Agranular + FI**	**Total Insula**
H9-88	21	Male	108.7	68.2	76.7	82.9	79.0
MU-88-65	50	Male	72.2	62.3	100.9	106.4	73.8
SN207-84	75	Male	127.1	76.0	84.6	85.9	87.8
W2-2-70	25	Male	113.4	101.0	62.8	73.7	94.1
STD-IIA-54	32	Female	86.2	54.7	27.0	40.3	56.6
		Mean	101.5	72.4	70.4	77.8	78.3

Table 6

Comparison of fold-differences in the sizes of neocortical areas between humans and the common chimpanzee (*Pan troglodytes*) and bonobo (*Pan paniscus*). Data appearing in bold refer to the data from the present study. All data are from either *in vivo* MRI or shrinkage-corrected measurements of histological sections.

Structure	*H. sapiens* versus *P. troglodytes* fold-difference	*H. sapiens* versus *P. paniscus* fold-difference	*P. paniscus* versus *P. troglodytes* fold-difference	Data source
Brain	3.6	4.0	0.9	Holloway (1996)
Neocortical gray	4.0	4.1	1.0	Rilling and Insel (1999)
Agranular insula without FI (right)	**10.0**	**4.3**	**2.3**	This study
Agranular insula without FI (left)	**7.3**	**3.4**	**2.1**	**This study**
Agranular insula and FI (left)	**7.2**	**3.3**	**2.2**	**This study**
Agranular insula and FI (right)	**7.2**	**3.7**	**1.9**	**This study**
FI (left)	**6.8**	**3.1**	**2.2**	**This study**
Area 44 (left)	6.6	–	–	Amunts et al. (1999), Schenker et al. (2010)
Area 10 (right)	6.3	5.1	1.2	Semendeferi et al. (2001)
Area 45 (left)	6.0	–	–	Amunts et al. (1999), Schenker et al. (2010)
Area 45 (right)	5.0	–	–	Amunts et al. (1999), Schenker et al. (2010)
Dysgranular insula (right)	**4.7**	**3.5**	**1.3**	**This study**
Total insula (right)[a]	**4.6**	**3.9**	**1.2**	**This study**
Dysgranular insula (left)	**4.2**	**3.2**	**1.3**	**This study**
Area Tpt (left)	4.2	–	–	Galaburda and Sanides (1980), Spocter et al. (2010)
Area 44 (right)	4.1	–	–	Amunts et al. (1999), Schenker et al. (2010)
Total insula (left)[a]	4.0	**3.8**	**1.1**	**This study**
FI (right)	**3.2**	**2.4**	**1.3**	**This study**
Granular insula (right)	**3.1**	**5.3**	**0.6**	**This study**
Granular insula (left)	**2.8**	**7.2**	**0.4**	**This study**
Area 6 (hemisphere unknown)	2.5	–	–	Glezer (1958),[b]
Area Tpt (right)	2.0	–	–	Galaburda and Sanides (1980), Spocter et al. (2010)
Area 17 (left)	1.8	1.3	1.4	de Sousa et al. (2010)
Area 13 (right)	1.4	3.3	0.4	Semendeferi et al. (1998)
Area 4 (hemisphere unknown)	0.8	–	–	Glezer (1958),[b]

[a] Includes all subregions of insular cortex (granular, dysgranular, and agranular insula and FI).

[b] All comparisons are based on volumes, except for the data from Glezer (1958), which provide surface area measurements.